HAL
open science

Morphology of fore-reef slopes and terraces, Takapoto Atoll (Tuamotu Archipelago, French Polynesia, central Pacific): The tectonic, sea-level and coral-growth control

Lucien F. Montaggioni, Antoine Collin, Dorothée James, Bernard Salvat, Bertrand Martin-Garin, Gilles Siu, Marguerite Taiarui, Yannick Chancerelle

To cite this version:

Lucien F. Montaggioni, Antoine Collin, Dorothée James, Bernard Salvat, Bertrand Martin-Garin, et al.. Morphology of fore-reef slopes and terraces, Takapoto Atoll (Tuamotu Archipelago, French Polynesia, central Pacific): The tectonic, sea-level and coral-growth control. Marine Geology, 2019, pp.106027. 10.1016/j.margeo.2019.106027 . hal-02276200

HAL Id: hal-02276200

https://hal.science/hal-02276200v1

Submitted on 20 Dec 2021

HAL is a multi-disciplinary open access archive for the deposit and dissemination of scientific research documents, whether they are published or not. The documents may come from teaching and research institutions in France or abroad, or from public or private research centers.

L'archive ouverte pluridisciplinaire **HAL**, est destinée au dépôt et à la diffusion de documents scientifiques de niveau recherche, publiés ou non, émanant des établissements d'enseignement et de recherche français ou étrangers, des laboratoires publics ou privés.

Distributed under a Creative Commons Attribution - NonCommercial 4.0 International License

Version of Record: https://www.sciencedirect.com/science/article/pii/S0025322719301732
Manuscript_c4eefe0fb79543d5c200ffb564b03c2d

Morphology of fore-reef slopes and terraces, Takapoto Atoll (Tuamotu Archipelago, French Polynesia, central Pacific): the tectonic, sea-level and coral-growth control

Lucien .F. Montaggioni [a,*], Antoine Collin [b], Dorothée James [b], Bernard Salvat [c], Bertrand Martin-Garin [a], Gilles Siu [d], Marguerite Taiarui [d], Yannick Chancerelle [d]

[a] *Aix Marseille Univ, CNRS, IRD, Coll France, CEREGE, 13331 Marseille, France*

[b] *PSL-École pratique des hautes études (EPHE), CNRS 6554 LTG, Labex Corail, Dinard, France*

[c] *PSL-École pratique des hautes études (EPHE), CNRS, UPVD, USR3278, Labex Corail, Université de Perpignan, 66000 Perpignan, France*

[d] *PSL Research University: EPHE-UPVD-CNRS, USR 3278 CRIOBE BP 1013, 98729 Papetoai, Moorea, French Polynesia*

[*] *Corresponding author*

Email address: montaggioni@cerege.fr

Postal address:

Aix–Marseille université

CEREGE UM 34

Saint-Charles

CS80249 (case 67)

3, Place Victor Hugo

© 2019 published by Elsevier. This manuscript is made available under the CC BY NC user license
https://creativecommons.org/licenses/by-nc/4.0/

F-13331 Marseille cedex 3

Abstract

A dataset of 41 bathymetric profiles detected by satelline imagery and echo-sounding to a maximum depth of 38 m along the fore-reef slopes of Takapoto Atoll (Tuamotu Plateau, French Polynesia, central Pacific) were qualitatively and quantitatively analyzed in order to identify the main geomorphological features. In addition, scuba-diving investigations from a selected site resulted in defining coral composition and cover rate. Six distinct fore-reef sectors were morphologically differentiated on the basis of seaward extension and slope gradient. Only the north end, and a restricted area of the mid-south-east side extend seawards over an average distance of 150 m, with a relatively low gradient (23°–38°). Most of the outer-slope areas are narrow (less than 100 m on average) and steep (average slope equals to 45° to up to 70°). Geomorphic features include spur-and-groove systems, sub-horizontal to gently dipping terraces (23–45 m wide) ending seawards in vertical steps (< 10 m high) and drop-offs (> 10 m high), outer-reef crest-like reliefs (0.5 m–1.5 m high), pinnacles (2 m–17 m high), coral heads (< 2 m high), trenchs and concave scars. The recognized seven terrace levels occur at the respective depths of about −5 m, −10 m, −15 m, −20 m, −24 m, −30.5 m and −38 m. Based on comparison with

subsurface chronostratigraphy of drilled reef sequences from some other Pacific atolls, the terraces are interpreted as remnants of reef tracts formed during Pleistocene interglacial, high sea-stands, respectively during MIS substage 5e (about −125 ka), MIS substages 7a (about −195 ka), 7c (about −210 ka), 7e (about −240 ka) and 9e (−330 ka). After depth correction of ground lowering during periods of emergence and subsidence effects, terrace elevations were expected to indicate eustatic sea-level positions at each identified high sea-stand, at approximately 7 m (MIS 5e) and 2.2 m (MIS 7a) above present sea level and 9.5 m (MIS 7c), 11 m (MIS 7e) and 8.6 m (MIS 9e) below present sea level. During the post-glacial sea-level rise, from about 9.5 ky, the studied portions of fore-reef slopes were re-flooded. It was assumed that coralgal deposits in the form of thin veneers, coral heads, outer-reef crest-like reliefs and pinnacles have simply overlapped pre-existing structures. Locally, the fore-reef zones are carved by trenchs, i.e. incipient detachment faults, and scars, i.e. imprints of former landslides. Similarly, some drop-offs may be regarded as fault walls. The prevailing direction of faulting–collapsing surfaces is consistent with the SW–NE orientation of the main axis of the atoll and submarine ridges rising up from the north-western floor of the Tuamotu Plateau. Analysis of the composition and distribution of coral communities to −30 m depth revealed high, downslope-increasing coral coverage (24 % to 67 % on

average) and the sharp replacement of robust-encrusting *Pocillopora* by sub-massive to plate-like *Porite*s from depths greater than −10 m. Significant inter-regional differences were detected with atolls in west Pacific, probably due to local ecological constraints.

Highlights

- A detailed survey of morphological features of upper fore-reef slopes from a Pacific atoll is provided for the first time, using satellite-based records.
- Five submerged terrace levels among the seven detected are regarded as related to distinct Pleistocene high sea stands are identified.
- At a large scale, the morphogenetic evolution of the atoll fore-reef slopes is mainly controlled by SW–NE trending regional-scale, tectonic structures.
- At a small scale, living coral communities with low diversity, but high cover contribute significantly to atoll fore-reef shaping.

Keywords: submerged terraces, fore-reef slopes, Pleistocene high stands, atoll, central Pacific.

1 Introduction

Coral reefs, typical ecosystems of many tropical coastlines, are known to be reliable indicators of climate, environmental (see Montaggioni and Braithwaite, 2009; Phinney et al., 2013 for reviews) and relative sea-level changes (see reviews by Montaggioni and Braithwaite, 2009; Murray-Wallace and Woodroffe, 2014; Woodroffe and Webster, 2014; Camoin and Webster, 2015). Intensive submarine exploration has given evidence that reefs have developed at times of lower sea levels, and at present located along continental and island shelves at different depths. A number of submerged reefs were described in the Pacific Ocean (Australia: Abbey et al., 2011; Webster et al., 2009; Linklater et al., 2015 – French Polynesia: Montaggioni et al., 1987; Cabioch et al., 2008; Camoin et al., 2012; Seard et al., 2013 – Hawaii: Faichney et al., 2009, 2010 and references herein – Papua New Guinea: Webster et al., 2004b; Ryukyus: Arai et al., 2016), in the Indian Ocean (Dullo et al., 1998; Rovere et al., 2018; and references herein) and the western Atlantic (Lightly et al., 1978; James and Ginsburg, 1979; Blanchon et al., 2002; Khanna et al., 2017; and references herein). Submerged reefs have proven to provide valuable information on relative sea-level and tectonic histories (Webster et al., 2004a,b, 2006; Cabioch et al., 2008; Faichney et al., 2010; Abbey et al., 2011; Rovere et al., 2018) and sub-aerial erosional patterns as well (Purdy and Winterer, 2001).

The origin of submerged reefs and associated topographic anomalies – terraces, breaks-in-slope, pinnacles and steps , has been intensively discussed (Hopley, 2006; Beaman et al., 2008; Abbey et al., 2011; Rovere et al., 2018). Reef tracts were speculated to form during either the last deglacial sea-level rise (–20 ka to –8 ka) or early, during late to mid-Pleistocene variations of sea level. They may be multi-generational, resulting from stacked successive growth and erosional episodes over several cycles of submergence and sub-aerial exposure, finally overlain by last deglacial deposits. Especially, terraces are interpretated to be constructional in origin or to have been shaped by erosive wave action during sea-level sea-stands lower than present. Similarly, steps may result from seaward accretional processes during stillstands, step and drop-off recession during low stands or faulting. Contrary to shelf slopes of continents and high volcanic islands, those of atolls have been little explored. Earlier bathymetric surveys using single beam echo-sounding have been conducted from the end of the forties on a number of Pacific atolls (Ladd et al., 1970; Winterer, 1976; Smith et al., 1994; Wong et al., 1999). Recently, investigations using shallow-water multibeam mapping, multispectral satellite-, optical- and acoustic-based imagery off several atolls from Pacific US overseas territories, provided new detailed insights into shelf morphology (for instance, see Poppenga et al., 2018). In French Polynesia,

shallow-water (0 to −30 m) bathymetric investigations were initiated at Moruroa (Chevalier et al. 1968).. At Takapoto, the first underwater surveys were carried out by Kühlmann and Chevalier (1986). A series of terraces and breaks-in-slope occur at different depths to about −40 m downslope. From satellite-derived near-shore bathymetry, Collin et al. (2018) provided the first high-resolution outer-slope morphometry of the eastern side of Takapoto.

In addition to geomorphology, the characterisation of coral communities living along the upper fore-reef slopes is an important step in terms of paleo-water depth reconstructions. The earlier works on the compositional and distributional patterns of coral communities at Takapoto were carried out by Chevalier and Denizot (1979), Kühlmann (1982), Bouchon (1983) and Kühlmann and Chevalier (1986).

In this study, are presented both morphological and biological datasets from the foreslopes of Takapoto Atoll in the Tuamotu Archipelago (French Polynesia, south-central Pacific). Analysis of satellite-based datasets gains insight into the detailed spatial distribution of submerged geomorphic features. Scuba-diving investigations reveal richness and cover rate of coral populations.

The aims of this study are to: (1) identify the main geomorphic features present on the shelf slopes and quantitatively describe their morphology; (2) define the depth distributional trends of

these features, especially those of terraces; (3) explore scenarios of their possible nature, mode and timing of formation, based on chronostratigraphic comparisons with other atoll sites; (4) determine the main depth-related compositional and distributional attributes of coral communities.

2 Environmental setting

2.1 Geological background

French Polynesia lies in the south-central Pacific and extends over about 5 500 000 km^2, from 134°28'W to 154°40'W and from 7°50'S to 27°S (Fig. 1a). Its sea floor includes a broad zone, the so-called 'Pacific Superswell' which is 250 to about 1000 m shallower compared to the depth predicted for its age by classical seafloor subsidence models (McNutt and Fischer, 1987; McNutt, 1998; Adam et al., 2014). It is typified by a great number of volcanoes, aseismic volcanic plateaus and seamounts, aligned along south-east to north-west linear (N115°E) trends, consistent with the predicted direction of absolute motion of the Pacific plate (Duncan and Clague, 1985). By contrast, the underlying oceanic crust exhibits structural features, including south-west to north-east-oriented, transform faults and magnetic lineations (Patriat et al., 2002) and volcanic ridges (Jordahl et al, 2004), and thus, oblique to the hot-spot-generated island trails (Ito et al.,1995) .

The Tuamotu Plateau, part of the oceanic superswell, encompasses an area of approximately 1500 km long and 800 km large (Fig. 1b). It does not exceed 2000 m in bathymetry and is composed of basaltic flows, postulated to have erupted near the East Pacific spreading centre. The plateau is known to be aged of 70 (Okal and Cazenave, 1985) to less than 50 million years (Schlanger et al., 1984).

Accretion of the north-west atoll-bearing volcanoes is attributed to the passage of two hotspots 50–30 million years ago as they migrated beneath the Pacific plate. However, the morphology and orientation of a number of linear volcanic features onto the plateau were controlled by tectonic structures of the underlying lithosphere. (Ito et al., 1995). Carbonate deposition over the oldest volcanoes is likely to have begun as early as 49 million years (Jackson and Schlanger, 1976).

2.2 Location of the study area.

Located between 14°33'S–14°43'S and 145°08'W–145°16'W, Takapoto Atoll rises from the northwestern portion of the Tuamotu Plateau (Fig. 1b). Its total surface area is 74 km², about 17 km long and 5.5 km wide. The atoll is elongate, oriented NE–SW, with an approximately 350 m wide rim enclosing a –45 m-deep lagoon. The outer part of the atoll rim is a living reef system, subdivided into three zones, from the sea inwards (Chevalier et al., 1979; Salvat, 1981; Salvat and

Richard, 1985; Laboute, 1985; Kühlmann and Chevalier, 1986; Montaggioni, 1981, personal observation). The outer reef zone comprises a spur-and-groove system, extending downwards to about 6–10 m, followed by sub-horizontal to gently sloping terraces to depths of 10–15 m, previously interpreted as the top of the last interglacial high-stand reef (Montaggioni et al., 2018). Below this, low gradient to sub-vertical slopes are developing to depths greater than 60 m. The emergent, innermost parts of the spurs are capped by an algal crest, about 20 m wide, reaching 0.20 m to 0.50 m above low tide level.

The climate in the northern Tuamotu is tropical, warm and humid. The rainy, austral summer lasts from November to April and the relatively cooler, and dryer, austral winter from May to October. Air temperatures vary between 23 °C and 30 °C. Annual rainfall averages 1500 mm. Tides are a twice daily regime and microtidal, 0.5 m in average amplitude and 0.70 m in maximum at spring tide. As in all Tuamotu islands, Takapoto is influenced by the south-east trade-winds, blowing from the ENE sectors for 70 % of the year and for 20 % from the SE sector. In the austral winter, 2.5-m high swells are generated by strong trade-winds. During the austral summer, trade-winds are significantly less active and generate moderate-energy wave conditions, locally disturbed by storm events initiated either by ENSO-related cyclones or by storms originating from northern latitudes (Andréfoüet et al., 2012).

The eastward migration of warmer sea surface temperatures during ENSO episodes promotes the displacement of tropical storms further east into the Tuamotu region (Larrue and Chiron, 2010).

Little is known about frequency of extreme wave hazards, i.e. tropical cyclone- and tsunami-generated. Over periods of several centuries, the number of cyclonic events has probably not exceeded 2–3 per century. The effects of cyclones and storms in shaping atoll morphology at the long-term scale is poorly documented (Montaggioni et al., 2018) onto atoll surfaces (Harmelin-Vivien and Laboute, 1986). Similarly, there is little information about the frequency of tsunami occurrences in the Tuamotu. Based on numerical modelling and direct observations, the Tuamotu islands seem not to have significantly suffered from tsunami impacts compared to some high-volcanic islands in French Polynesia (Sladen et al., 2007).

3 Methods and data

3.1 Acquisition and analysis of geomorphic data

Pleiades-1 satellite imagery was collected over Takapoto Atoll on September, 22 2016 at 20 h 01 min 03 sec (UTC). Orbiting at 694 km altitude, Pleiades-1 sensor provides four spectral wavebands (blue: 430 nm–550 nm, green: 490 nm–610 nm, red: 600 nm–720 nm, and infrared: 750 nm–950 nm) at 2 m pixel size. The processed imagery totaled 72 294 672 pixels in

the form of 9759 lines and 7408 columns. Given the sun-sensor-scene trigonometry, a geometric correction was necessary to project multispectral imagery in UTM 6 South within RGPF local datum. For the sake of standardization and further comparison, a radiometric correction was carried out. It firstly converted top-of-atmosphere (TOA) digital number into TOA radiance using calibration factors, secondly TOA radiance into down-of-atmosphere (DOA) radiance by compensating for atmosphere absorption, and thirdly DOA radiance into DOA reflectance by sun irradiance normalization.

In parallel, a sonar campaign, aiming at calibrating–validating a depth model, was conducted, from September, 25 to 26, 2016, to acquire water depth soundings over both lagoon and ocean parts (Fig. 2a). Fieldwork week was close enough to imagery date to be confident with an absence of bathymetric disturbances between two periods. An array of 276 082 geolocated measurements was compiled across 104.4 km over 16 h 44 min recordings. The dataset ranged from 0.54 m to 180.85 m with an average of 9.90 m ± 10.02 m. The sonar device, installed on a fishboat, was a 200 kHz echosounder Lowrance HD7 leveraging a 10 Hz GPS unit. Water level driven by tide was corrected using the nearest French Marine gauge in Rangiroa atoll.

The bathymetry has been extracted based on the optical law, showing that electro-magnetic radiation is absorbed by water in

respect to the wavelength. Pleiades-1 infrared waveband enabled to discriminate land from sea areas, owing to the strong water absorption of the infrared. Three remaining visible Pleiades-1 wavebands (blue, green and red) were used to elucidate the bathymetry based on the ratio transform (Stumpf et al., 2003):

$$Z = a_1\left(\frac{\ln(R_w(\lambda_i) - R_\infty(\lambda_i))}{\ln(R_w(\lambda_j) - R_\infty(\lambda_j))}\right) - a_0 \qquad (1)$$

where a_0 is the intercept for a null water depth (0 m), a_1 is the modeled slope converting the ratio to absolute bathymetry, R_w is the DOA reflectance related to the waveband λ_i, and R_∞ is the DOA reflectance above no-bottom water. Both intercept and slope stemmed from soundings, whose values were re-adjusted by an offset linked with the tide level observed at the satellite collection time.

A very strong agreement between waterborne sonar observations and spaceborne modeled depths was reached ($R^2 = 0.95$, RMSE = 0.17 m, see Collin et al. 2018 for more details). Since the model accuracy declined with depth, a truncature at 38 m was applied. The formula, underlying the model, was thereafter implemented to every pixel, in order to build a digital depth model spanning the entire scene captured by the satellite.

Finally, a set of 41 bathymetric profiles was selected (Fig. 2b) and visually inspected to define the type and spatial distribution

of morphological features imaged on the atoll shelf slopes. Especially, criteria used to define terraces include the identification of flat-topped to low-gradient surfaces and major breaks-in-slope across the island shelves. The geomorphic features are classified according to their sizes, from larger-scale (hectometres to kilometres) to finer-scale (metres to decametres). The geomorphological classification used in this study is adapted from previously published descriptions and in common usage (see Beaman et al., 2008 and Addey et al., 2011 for reviews). Table 1 and figures 2b and 3 present the different geomorphic features.

Shelf-slope inclination and size, elevation and width of the different geomorphic features were manually measured from the recorded transects. To measure terrace width, slope extension and inclination, and graphically compare the depth ranges of the successive terrace levels, positive reliefs, such as pinnacles and coral heads, were masked.

3.2 Acquisition and analysis of biologic data

The study site is located at the south end of the atoll, close to the village of Fakatopatere and profile T23. Digital images of the quadrats were acquired using a SLR Nikon D300s body camera with aquatica housing and equipped with a Nikkor 15 mm (AF 15 mm *f* / 2.8) lens and two SB 105 Nikonos strobes. Pictures were taken at –5 m, –10 m, –15 m, –20 m, –25 m, and

–30 m depth running downslope. At each depth site, 4 pictures were taken perpendicular to the bottom surface with a frequency of 1 picture every 30 seconds by a scuba diver swimming at low speed (1 m per 5 sec). Reef bottom to camera lens distance was approximately 5 m. Digital pictures were processed on computer screen using the point intercept method (50 points–picture). Frequency of coral/non-coral substrate was assessed on each picture by identifying the benthic category present under each point. Except in some cases, coral taxa were identified at the genus level. Amount of living coral cover was obtained by calculating the proportion of points occupied by living coral colonies against the total number of points in a given processed surface area.

4 Results

4.1 Morphometry of fore-reef features.

Visual examination of the 41 bathymetric profiles (T1 to T41) revealed significant variability in distribution, shape and size of fore-reef features.

4.2 Gross morphology

Six morphologically distinct sectors can be delineated around the atoll, based on seaward extension and mean slope gradients of the bathymetric profiles (Figs. 4 and 5).

The north-end sector (T1 to T5) appears to be the widest with deepest points at 30 m to 36 m, at a distance of 143 m to 190 m from the modern reef-crest line (Fig.4a and 5a). It has relatively gently dipping slopes (23° to 38°) and numerous sub-horizontal terraces, 7 m to 45 m wide. Usually, terraces terminate in steps, 1.80 m to 10 m high. There is a prominent line of pinnacles, with elevations of 2.70 m to 17 m.

The eastern sector (T11 to T16) exhibits steeply dipping slopes (45°–58°) punctuated by narrow (less than 15 m) terraces ending in steps, 2 m to 15 m high (Figs. 4b and 5b). The deepest points are at 30 m to 37 m, 80 m to 110 m far from the modern reef-crest line. Pinnacles are usually rare or scattered, and not exceed 3.50 m in average elevation. Coral heads are occasional.

The south-end sector (T19 to T25) is characterized by steeply dipping slopes (45°–65°) frequently ending in vertical drop-offs (Figs. 4c and 5c). The lowest depths recorded range between 26 m to 36 m, at the distance of 70 m to 135 m from the modern reef-crest line. Terrace width varies between 3 m and 15 m. Step height ranges from 2 m to 17 m. Pinnacles are absent or uncommon.

The north-western sector (T31 to T41) exhibits a gradient of 45° to up to 70°. The deepest points recorded range between 6 m and 24 m, at 80 m to 105 m far from the reef front line.

There are successive, narrow terraces (2 m–15 m wide) and low steps (1.80 m–12 m). Pinnacles and coral heads are occasional.

The steepest foreslopes are located in the north-eastern and south-western sectors of the atoll (T6 to T10 and T26 to T30, respectively) (Fig. 4e and 5e). The mean slope angle varies between 64° and up to 75° (Fig. 6). Along the north-eastern margin, the base of the profiles does not exceed depths of 26 m to 36 m, at the distance of 40 m to 55 m from the modern reef-crest line. Along the south-western side, the deepest detected isobath ranges between 9.5 m and 14 m only, at a distance of 40 m–50 m from the modern outer reef-crest line. In both sectors, the slope is interrupted by narrow terraces, usually less than 7 m wide ending in low steps and drop-offs, ranging from 2 m to 15 m in elevation. The height of pinnacles does not exceed 8.5 m. Coral heads are common.

There is locally an atypical zone at the mid-south-eastern side (T17, T18) along which a gently dipping (25°–35°) slope ends in drop-offs not higher than 7 m (Fig. 4a and 5e). The zone between the reef crest and the 38 m isobath extends for a length of 120 m to 210 m. Pinnacles are common, with heights of 2 m to 4.80 m.

4.3 Terrace levels.

The morphology of the Takapoto outer-reef slopes is typified by several sets (or levels) of terraces. These lie at relatively

recurrent depths from the sea surface to about 38 m and have a relatively spatial continuity. Seven morphologically distinct levels of terrace (TL1 to TL7) were recognized (Fig. 7).

4.3.1 Terraces TL1

As in most of reef zones facing the open ocean, the outer reef crest extends into a seaward dipping terrace, which is the top surface of the spur-and-groove system (Fig. 8). Locally, this terrace is missing or poorly developed, ending in abruptly dipping (50°–76°) or vertical drop-offs, especially along the north-eastern, eastern (windward) and south-western (leeward) sites. This means that the development of the spur-and-groove system is not directly dependent upon the location and orientation of the foreslopes, since locally lacking from both some windward and leeward sectors. The main driving factor seems to the slope angle; spurs and grooves are usually restricted to more gently dipping slopes, irrespective of exposure to winds and waves. At its seaward end, the depth of TL1 edges range between 2 m and 7 m, with an average depth of 5.24 m ± 2.0 m.

4.3.2 Terraces TL 2

This terrace, identified from 34 profiles, is found at the average depth of 10.1 m ± 2.4 m (Figs. 6, 8). It is missing from narrow, steeply dipping slopes and drop-offs (profiles T6 to T10, T22,

T23, T27 to T30). The surfaces seem generally to have a bumpy morphology generated by thick and widespread coral layers or metre-high coral heads, locally oriented perpendicular to the terrace margins. In most cases, the seaward margin of TL2 ends in a steep break-in-slope. Another point to note is the presence of outer reef-crest-like morphologies, less than 2 m high, at the seaward margin of the terraces.

4.3.3 Terraces TL 3

On 28 profiles, a third set of terraces is identified at an average depth of 14.7 m ± 3.8 m. These terraces are missing from a number of transects because of local strong steepness (T4, T8, T9, T10, T20, T26 to T33, T37, T39 to T41).

4.3.4 Terraces TL4

Another level of terraces is encountered at an average depth of 20.3 m ± 2.3 m on 20 out of the 41 profiles. Yet, the strong steepness of the fore-reef slopes makes the mid-fore-reef zone deeper than 20 m not accessible, as seen on T21 to T30, T33, T34, T35, T36, T39 to T41. Despite high coral cover rate, the occurrence of TL4 can be inferred from T17 to T20 based on sharp changes in slope.

4.3.5 Terraces TL5

The relevant terraces are found from 21 sites at an average depth of –24 m ± 2 m. These are missing from the transects T6, T13 à T17, T26 to T41.

4.3.6 Terraces TL6

These terraces are inferred from seven profiles showing gently shelving surfaces (T3, T11, T14 to T17, T20, and T23) and located at an average depth of 30.5 m ± 3 m.

4.3.7 Terraces TL7

The deepest terrace recorded is at 38 m, only from T17 and T18. Examining patterns among profiles show similarities and contrasts in the number and width of terraces. In order to determine the number of terraces within a given width range, a frequency histogram was generated (Fig. 9). Among the 112 terraces identified from the 41 profiles, most have widths less than 20 m.

Furthermore, the width of terraces appears to be partly correlated to the length of profiles (Fig. 10) which is slope-gradient dependent. Where profile lengths do not exceed 80 m, most terrace widths are less than 8 m. On profiles as long as 100 m–110 m, a number of terraces can be as wide as 15 m to 20 m. The profiles longer than 130 m have one-quarter of their terraces, 25 m to 45 m wide.

4.4 Pinnacles

Steep-sided, high reliefs, found on terraces, were interpretated as isolated pinnacles. These are widepread along gently inclined slopes (profiles T1 to T6), but less common on steeply dipping slopes. Their elevation and diameter range from about 2.30 m to 15 m and 2 m to 12 m respectively. However, it is neccessary to remain cautious about inferring the possible lateral extent of a pinnacle line from transects.

4.5 Drop-offs, trenchs, and scars

Drop-offs of 11 m to 13 m high are encountered at several shelf locations (T13, T19, T21, T26, T27, T32, T37) at different depth ranges, from −9 m to −35 m deep. Trenchs are observed on profiles T24 and T31 (Fig. 5d), in the form of 6 m to 17 m-deep indentations, at depths of −6 to −12 m and −12.5 to −29.5 m respectively. Concave scars, interpreted as collapsed margin portions, are found at the south-eastern side and along the western side of the atoll (Fig. 2a).

4.6 Quantitative assessment of coral communities

Living coral cover increases downslope from 24 %–25 % at depths of −5 m and −10 m to 42 %, 55 %, 67 %, and 50 % at depths of −15 m, −20 m, −25 m, and −30 m respectively (Table 2, Fig. 11). Robust-branching *Pocillopora* (mainly, *P. verrucosa*) is the dominant genus at the upper fore-reef

settings, representing 10 % to 26 % of coral coverage, from −5 m to −10 m deep. At depths of −25 m to −30 m, pocilloporids do not exceed 2 %–4 %. Sub-massive to plate-like *Porites* (*P. rus*) becomes the prominent coral form from 15 m deep, locally covering 50 % to up to 85 % of the substrate. Other scleractinian corals belong to *Acropora, Porites* cf. *lobata, Leptastrea*, and *Montipora*, each of them not exceeding 2 % to 4 % of the total coral cover. It is noteworthy that along steeply dipping slopes and drop-offs, modern coral buildups have significantly re-shaped antecent substrate morphology (Fig. 12)

5 Discussion

5.1 Mode and timing of terrace formation

As pointed out by Rovere et al. (2018), in absence of radiochronological constraints, the age and formational patterns of marine terraces remain speculative. However, different possible scenarios for their mode and timing of formation can be discussed, especially since two processes, respectively constructional or erosional, may have been involved in terrace shaping, either prior to the last glacial maximum (−23 ka to −20 ka-interval) over the past 300 ky or afterwards, during the last deglaciation.

From a contructional point of view, most submerged terraces identified in this study, especially those from gently sloping

shelves (profiles T1 to T5, T17, T25, T35) may have developed according to one of the two following models. First, these may result from backstepping of reef bodies developed during the last deglacial rising sea level or previous deglaciation times. In these cases, reef-related terraces would have been generated by punctuated sea-level jump events that have forced reef bodies to drown and backstep upslope through time, rather than develop upwards from a gradual and continuous sea-level rise. Secondly, the terraces may have been shaped during one of high sea-stands that have occurred over the late to mid-Pleistocene. In all scenarios, terraces represent the still visible, outermost surfaces of reef edges of former reef tracts.

From an erosional point of view, submerged terraces may result from marine planation during episodes of slowing in sea-level rise or stillstands during the last deglaciation. In this scenario, terraces would be wave-cut platforms, as suggested in the Maldives for the last deglaciation (Rufin-Soler et al., 2013; Green et al., 2014).

At Takapoto, as everywhere in French Polynesia, during the post-glacial transgressive phase, sea was at a level corresponding to the deepest isobath recorded in the profiles (−38 m) by −9.5 ka. Sea level continued to rise at a rapid and relatively constant rate of $10\ \mathrm{mm} \cdot \mathrm{y}^{-1}$ before reaching its present position by about −6 ka (Bard et al., 1996, 2010). Slowly rising sea level is known to provide the much-needed

accommodation space for enhanced vertical reef accretion while lateral accretion is dependent of the relative time spent at sea level. According to the mean vertical reef accretion rates (4–5 mm · y^{-1}) estimated for the early Holocene (see Dullo, 2005; Montaggioni, 2005; Hubbard and Dullo, 2016; Gischler and Hudson, 2019, for reviews), the rate of sea-level rise was most likely too high to allow coral growth to maintain pace with sea level or to prograde oceanwards. As observed on the mid-shelf slopes at Tahiti (**Seard** et al., 2013), during the post-glacial transgression, corals have rather built isolated, straight-walled pinnacles or thin veeners covering the Pleistocene antecedent topography than typical, flat-topped fringing reefs. A similar scheme was described from Mayotte Island (Comoros, Western Indian Ocean) by Dullo et al. (1998). By analogy, at Takapoto, the major morphological characteristics of the fore-reef slopes are assumed to dominantly reflect those of the antecedent substrate upon which coral buildups have grown more recently. Accordingly, the core of most terraced structures is probably late to mid Pleistocene in age. The heigth of steps is probably indicative of the thickness of the related reef unit. Additionally, a sea-level rise at the rate of 10 mm · y^{-1} appears inappropriate to allow shelf slopes to be abrased or excavated. Similarly, during the penultimate (from MIS 6b to MIS 5e) and oldest (MIS 10 to MIS 9, MIS 8 to MIS 7) deglaciation episodes, sea level rose at rates similar to or higher

than those recorded from the last deglaciation (Siddall et al., 2007), precluding any significant constructional, abrasional or excavational event to have occurred. Accordingly, the identified terraces and associated reef units were assumed to have formed during high sea stands.

Some terraces possess outer crest-like reliefs of 0.5–1.5 m in elevation and 3–6 m in width at the seaward margin (for intance, see Fig. 5a, b). Given their specific location on top of the outermost part of submerged reef edges, these features are interpreted to be isolated coral heads or laterally extending, continuous ridge-like, coralgal buildups developed at windward, high-energy settings during the Holocene course of sea-level. Contrary to most of pinnacles described along the shelf slopes at Takapoto, their upward development would have been drastically interrupted in response to the rapid sea-level rise. In some way, these are « give-up » reefal features in the sense of Neumann and Macintyre (1985). Morphologically speaking, these buildups are similar to windward, high-energy, coralline algal ridges (Adey, 1978, 1986; Montaggioni and Braithwaite, 2009), typical of Pacific atoll rims (Chevalier et al., 1969), particularly at Takapoto (Chevalier et al., 1979; Chevalier and Salvat, 1976). Submerged terraces with raised coralgal ridges at their outer extent are known from a number of Pacific reef sites: Australian Great Barrier Reef (Beaman et al., 2008; Abbey et al., 2011; Webster et al., 2018), Hawaii

(Webster, 2004a) and Papua New Guinea (Webster et al., 2004b, 2009), Ryukyu Islands (Arai et al., 2016) and the Marquesas (Cabioch et al., 2008). These terraces are thought primarily to be remnants of coralgal piles developed at the seaward margins of incipient fringing reefs during the post-glacial times, but not capable of keeping pace with rising sea level.

At Takapoto, terraces TL2 exhibit locally low, coral-built ridges oriented perpendicular to the reef-edge line and alternating with elongated, sand-filled grooves, similar to spurs-and-groove reliefs (Fig. 11b and Montaggioni, personal observations, 1981). Accordingly, TL2 are regarded as outer-reef edge features. By analogy, the terraces identified downslope (TL3 to TL7) may be also interpreted to be remnants of paleo-reef-edge surfaces.

Along both gently inclined terraces and shelf slopes, pinnacles are common (for instance, see Fig. 5a–f). These features were also described on a number of submerged tropical shelves, mostly on the Australian Great Barrier Reef where they are usually associated with modern juvenile reefs (Hopley, 1982). According to Abbey et al. (2011), during the last deglaciation, terraces would not be ideal settings for extensive vertical coral accretion, due to their narrowness. Similarly, at Takapoto, during the final course of the rising sea level, from about 9.5 ka, and despite the subsequent increase in accommodation

space, coral growth was unable to produce, flat-topped, aggrading reefs.

5.2 Faulting and submarine landslides

The present data reveal that, at both windward and leeward settings, except in its north extremity and mid-south-east, part the Takapoto rim is bounded by steep fore-reef slopes, with gradients up to 45° or vertical submarine cliffs. There are no significant differences in the overall fore-reef morphology between windward and leeward sides of the atoll. The steepest fore-reef slopes were found as well along the western, leeward coast as the eastern, windward one (Figs.4 and 5). This suggests that the swell regime from the east is not the main driver of foreslope evolution.

The atoll seaward margins are nearly linear as opposed to most of the curved high volcanic island margins found in the nearby Society and Marquesas archipelagos, thereby suggesting structural failure. Faulting control in shelf shaping is further supported by both the presence of vertical drop-offs, higher than 10 m, and trenchs, 6 m to 17 m deep, cutting through the upper parts of the shelf slopes. The trenchs are considered to be incipient, normal faults. Similar features were reported from Tikehau (Faure and Laboute, 1984), and Moruroa (Chevelier et al., 1969). The overall tectonic evolution of the Tuamotu plateau, appears to be partly driven by extensional processes in

relation to major, regional fracture zones. The fault distributional patterns of nearby, high-carbonate Makatea Island (Montaggioni, 1985) are quite similar, oriented in a south-west to north-east (35°N–50°E) direction. It is noteworthy that the lagoons of Takapoto and other atolls of the outer Northern most Tuamotu island-belt (Takaroa, Ahe, Manihi, Raroia, Takume), together with that of southermost Amanu atoll, are aligned according the same direction. These atolls are superimposed upon ridges, that are expected to have been formed from erupting fissures influenced by the underlying lithosphere fractures (Jordahl et al., 2004). The dominant fault system affecting the western and eastern shelf slopes at Takapoto is clearly oriented parallell to the atoll and ridge alignment. By contrast, the island shelves at the north end, which developed outwards at right-angles to the SW–NE fault system, have probably escaped large-scale collapsing, thus explaining their unusual morphology, i.e. large seaward development, high density of pinnacles and lack of high escarpments.

Scars in the normally convex seaward margins of atolls and reef barriers as well were usually interpretated as resulting from submarine landslides generated by slope failure (Fairbridge, 1950; Keating, 1987, 1998; Keating and McGuire, 2000; Riyaz and Park, 2008; Terry and Goff, 2012, 2017; Webster et al., 2016; Poupardin et al., 2017; Puga-Bernabéu et al., 2017). As

emphazised by Terry and Goff (2017), submarine landslides can significantly modify gross atoll morphology. In addition, giant landslides can generate tsunamis (Webster et al., 2016) and subsequent, partial submersion of atoll rims (Poupardin et al., 2017). Although rare, especially in the Tuamotu (Sladen et al. 2017), landslide-generated tsunamis can contribute to atoll shaping and island formation.

5.3 Significance of terraces in terms of sea level

In absence of a chronological frame, as a first approximation, the submerged terraces identified at Takapoto may refer to higher or lower Pleistocene sea-stands relative to present sea level. Hovewer, over the last 500,000 years, sea level during interstadials and glacial, low stands were systematically at depths greater than −30 m (see Murray-Wallace and Woodroffe, 2014 for reviews), especially at atoll-subsiding sites (Camoin et al., 2001). Accordingly, at Takapoto, all the terrace sets were assumed to refer to interglacial, high-sea stands.

Morphological and chronostratigraphical correlations between Takapoto and some other atolls used as reference sites in the Pacific can be attempted to help attributing a given terrace level to a specific highstand. All reference cores used herein were extracted from outer reef-flat settings (Fig. 13).

On Moruroa Atoll, there is an upper, gently sloping (10°) terrace, about 60 m wide, extending from about −4 m to −10 m deep. It is interrupted by a break-in-slope followed by a steeper (25°) mid-shelf topography (Chevalier et al., 1969). Similar morphologies were described from Enewetak and Bikini Atolls, Marshall Islands (Tracey and Ladd, 1974), Tarawa, Gilbert Islands (Marshall and Jacobsen, 1985) and Yongle Atoll, Xisha Islands, South China Sea (Guozhong et al., 1990). The break-in-slope at approximately −10 m deep was regarded as superficially translating the presence of an unconformity, i.e. subaerial exposure surface. This surface is encountered beneath the modern outer reef-flat and reef-edge zones at depths of −10 m to −14 m at Enewetak (Tracey and Ladd, 1974; Lincoln and Schlanger, 1991; Ristvet et al., 1977; Szabo et al., 1985), −8 m to −10 m at Bikini (Emery et al., 1954; Tracey and Ladd, 1974), −11 m to −17 m at Tarawa (Marshall and Jacobsen, 1985), and −16 m to −17.3 m at Yonge Atoll (Jian et al., 1997). Uranium-series dating of coral material collected above and below this unconformity revealed that this surface separates an overlying Holocene reef unit not older than 9 ka, from a late interglacial (MIS 5e) unit, dated at −120 ka ± 10 ka to −134 ka ± 5 ka, as observed in Moruroa, Enewetak, Bikini, and Tarawa (Fig. 13). The thickness of the Holocene reef sequences ranges approximately between 12 m and 17 m. At Takapoto, the uppermost reef unit, spur-shaped, approximates a maximun

thickness of 10 m. By analogy with the reference atolls, it is considered to be Holocene in age, probably not older than 9 ka.

On the basis of morphological and structural similarities between the upper parts of outer-edge zones among atolls, terraces TL2 were thougth to be geomorphic analogs of the unconformity surfaces atop of MIS 5e reef units. During the relevant high sea-level episode (−128 ka to −116 ka; Muhs, 2002), sea level was between 5.5 m to 9 m above psl (Dutton and Lambeck, 2012). Based on statistical modelling, there would have a 95 % confidence level that global sea level, irrespective of local controls, peaked at 6.6 m above psl and a 67 % probability that sea level was higher than 8 m above psl during MIS 5e, but it was unlikely to have been higher than 9.4 m (Kopp et al., 2009).

A second subaerial exposure surface was found in the same reference cores at Moruroa, Enewetak, Bikini and Yongle, at depths of −18 m to −22 m, −22 m to −23 m, −24 m to −27 m, and 30 m respectively (Fig. 13). The reef sequence capped by this surface yielded U-Th ages averaging −215 ka at Moruroa (Camoin et al., 2001) thus indicating that the relevant reefs have developed during the penultimate interglacial (MIS 7) high stand. No date is available from other atoll sites. On these atolls, the depth of the second unconformity relative to psl is locally greater than that of terraces TL3 (14.7 m ± 3.8 m), but closer to the level of terraces TL4 (20.3 m ± 2.3 m) and TL 5

(24 m ± 2 m). It is obvious that attempting to link the terraced surfaces TL3, TL4, and TL5 to MIS 7 substages result in significant uncertainties, in part, induced by differences in local erosional and tectonic patterns (see sections 4 and 5 stage). Among the reference atolls, the total thickness of reef units deposited during the entire MIS 7 stage is similar, varying from 11 m to 15 m. At Takapoto, the thickness of the intervals delineated by TL3–TL4, TL4–TL5, and TL5–TL6 range between 5 m and 7 m only. Such thickness values appear to be too low to account for the entire MIS 7 depositional history of Takapoto when compared to other atoll sites and with regard to the thermal subsidence constraints of the atoll (see section 5 below). On the contrary, integrating the whole TL3–TL6 depth interval (average = 16 m) provides a greater reliance on depositional patterns for the entire MIS 7 episode in the studied area. Furthermore, while there is often an inability to distinguish one substage to another within the penultimate and older interglacials from cored reef sequences (Camoin et al., 2001; Montaggioni et al., 2015), identification of distinct sea-level pauses from a series of closely stepped terraces seems achievable if assuming that terrace formation is the result of successive backstepping events during successive high-stand substages. Each terrace may correspond to the outer-edge surface of one single backstepped reef tract as observed in a number of reef provinces worldwide (Barbados: Fairbanks,

1979; the Marquesas: Cabioch et al., 2008 – Hawaii: Sanborn et al., 2010 – Texas: Khann et al., 2017 – Great Barrier Reef, Australia: Webster et al., 2018). Accordingly, the best interpretative scenarios for TL3, TL4, and TL5 are the following. These terraces may correlate respectively with MIS 7a (–201.5 ka to –189.7 ka), MIS 7c highstand (–217.2 ka to –206 ka) and MIS 7e (–248.9 ka to –231 ka) (Figs.13 and 14).

Few coastal landforms referring to MIS 9 (–335.6 ka to –316.8 ka), especially in reef provinces, are documented, most likely due to lower preservation potential and reduced accessibility (Murray-Wallace and Woodroffe, 2014). At Moruroa, a third solution unconformity was recognized in vertical cores between 29 m to 32 m below psl. It caps a 7–11 m thick, reef unit (Buigues, 1997). This unit is regarded as the lateral equivalent of reef-margin deposits recovered from oblique boreholes and dated at –332 ka ± 12 ka (MIS 9e substage) by Camoin et al., (2001). On Enewetak and Bikini, a third unconformity was penetrated at 36.2–42.5 m (Ristvet et al., 1977; Szabo et al., 1985), and at 49 m below psl (Tracey and Ladd, 1974) respectively. In the latter site, a coral sample from the underlying interval gave an age older than 400 ka, apparently inconsistent with local stratigraphy. To maintain consistency with the overall development history of Takapoto submerged terraces, TL6 are approximated to refer to MIS 9e.

The belonging of terraces TL7 to a given MIS stage is facing considerable uncertainty and therefore is not discussed.

5.4 Effects of subaerial erosion

Another prerequisite to define a paleo-relative sea-level position from given terrace levels is quantifying the impact of subaerial erosion on the morphological evolution of terraces during times of emergence. From estimates of the amount of reef rocks destroyed over the last 120 ky, the rates of carbonate ground lowering from some Pacific atolls and reliefs were thought to range between 0.011 mm · y^{-1} and 0.202 mm · y^{-1}, with mean rates of 0.11 mm · y^{-1} (Paulay and McEdward, 1990). These values are similar to those calculated (0.12 mm · y^{-1} on average) by Purdy and Winterer (2001) from Enewetak Atoll for the same time span in response to local rainfall regime. Since present-day annual rainfall at Takapoto is around 1500 mm · y^{-1}, quite similar to that recorded at Enewetak (Purdy and Winterer, 2001), a mean value of 0.12 mm · y^{-1} is taken as the maximum solution rate during Pleistocene low sea stands in the north-western Tuamotu.

5.5 Subsidence

In the Tuamotu, the thermal sinking rate of the underlying oceanic crust is lower than the usual decaying exponential rate (about 0.32 mm · y^{-1}–0.35 mm · y^{-1}: Menard, 1969; Korenaga

and Korenaga, 2008) as a function of increasing age as for most of oceanic volcanic domains (Patriat et al., 2002). The Tuamotu plateau. In relation to its age (47 to 55 million years old), the Tuamotu plateau is considered to be near isostatic equilibrium since it was emplaced (Patriat et al., 2002). Moreover, for the north-western Tuamotu islands, earth dynamic topography models predicted about 2–3 m fall since the last 125 ky, which is included in the subsidence signal (Austermann et al., 2017).

Quantitative constraints on the possible rate of subsidence at Takapoto can be provided on the basis of the following assumptions: (1) subsidence is expected to approximate linearity for the past 300 ky; (2) TL2- related reef unit formed during MIS 5e high stand; (3) at that time, sea level peaked at +7 m above psl (Rovere et al., 2016); (4) the rate of sub-aerial erosion averaged 0.12 mm · y^{-1}; (5) the time span during which MIS 5e reef was exposed lasted 106.5 ky, from 116 ka to 9.5 ka, i.e. from the termination of the MIS 5e substage to the time of re-flooding of the shelf slope from the deepest detected isobath. As a result, the ground lowering of the TL2-related reef pile during emergence can be estimated at around 12 m. If correct, given TL2 is now at about 10 m deep, the subsidence amplitude would be about 5 m. The calculated subsidence rate is 0.047 mm · y^{-1} for the past 125 ky. This rate is in complete accord with that estimated (0.045 mm · y^{-1}) from Pukapuka and Rakahanga Atolls (Gray et al., 1992), the origin of which is

linked to the formation of the Manihiki Plateau as old as the Tuamotu basement (Mahoney, 1987). Similar thermal subsidence rates, around 0.035 mm · y^{-1} to 0.050 mm · y^{-1} were inferred from other mid-plate low-lying carbonate islands originated during the early Cenozoic (Schlanger et al., 1987; Quinn, 1991; Gischler et al., 2008).

5.6 Identification of paleo-relative high sea-levels

Paleo-sea-level reconstructions over the last 300 ky were attempted to be achieved on the basis of the vertical distribution of terrace levels at Takapoto (Table 3). The rates of sub-aerial erosion (0.12 mm · y^{-1}) and thermal subsidence (0.047 mm · y^{-1}) previously determined were used in the calculations, assuming that similar environmental and tectonic conditions have prevailed during all considered high sea stands.

The position of a paleosea level at a given high stand (SL) was calculated as follows: $SL = S + E - TL$ where S is the product of the amount of time during which a given terraced-reef tract has subsided and of the subsidence rate, subsidence operating as soon as reef growth has initiated; E is the produit of the amount of time during which a given reef pile has been emerged and undergone ground lowering and of the erosion rate, considering that duration of emergence is the time interval between the termination of a given high stand and the start of the following re-flooding and subsequent overlapping by a new

reef generation. TL is the present depth at which a given terrace is found (Table 3).

Terraces TL3, as remains of MIS 7a reef surfaces, would have suffered a ground lowering of 7.40 m and a drowning of 9.50 m since they have formed, resulting in a deepening of −16.90 m relative to their initial position. Based on its present location at an average depth of 14.70 m ± 3.8 m, the paleo-sea level is estimated to have been at 2.2 m ± 3.8 m above psl. Regarding terraces TL4, as referred to MIS 7c, ground-lowering and subsidence amplitudes were assessed to be 1.20 m and 9.60 m respectively. The resultant drop did not exceed 10.80 m while these features are found at present at −20.30 m ± 2.3 m. This means that the related past sea level was at 9.50 m± 2.3 m below psl. Two alternative scenarios can account for the evolutionary history of MIS 7e reefs represented by terraces TL5. In the case where this reef generation was overlapped by younger MIS 7c reefs, the time of emergence has not exceeded 11 ky and the thickness of the reef pile released by solution ranged around 1.30 m. If sea level was lower, MIS 7e reefs may have remained exposed over 31 ky. Accordingly, ground lowering of MIS 7e deposits would reach 3.70 m. In both situations, subsidence was 10.30 m. The resulting terrace deepening ranges between 13.0 m and 15.40 m. Given terraces TL5 are now located at a depth of −24 m ± 2 m, the MIS 7e sea level may have been at approximately 11 m or 8.60 m ± 2 m

below psl. The morphological evolution of reefs TL6 is summarized as follows. Sub-aerial erosion would have removed 9.20 m while sinking motion was 15.80 m in amplitude. Finally, terraces TL6 were deepened by 25 m. With respect to their present depth location, the corresponding reef tops were believed to have originally cropped out at a paleo-sea level between 5.80 m ± 3 m below psl.

The past sea-level positions derived from fore-reef morphometry at Takapoto appear to be in good agreement with some predicted on the basis of different proxies in different seas (Fig. 14). Regarding the elevations at which sea level peaked during the MIS 7 substages, reconstructions gave evidence for only two prominent high sea levels, MIS 7a and 7e, close to or higher than present, between −12 m and +4 m relative to psl. These findings are based on U/Th dating of speleothems in Bahamian caves (Li et al., 1989; Lundberg and Ford, 1994), open-system uranium-series ages (Thompson et al., 2003; Thompson and Goldstein, 2005) and ESR ages (Schellmann and Radtke, 2004) of corals collected from uplifted reef terraces at Barbados, stratigraphic and radiometric constraints in the Bahamas and Bermuda (Hearty and Kindler, 1995), paired Mg/Ca and oxygene isotope measurements of planktonic foraminifera cooled in a core from the Cocos Ridge (Lea et al., 2002), sea water oxygen isotope in the Red Sea (Siddall et al., 2003) and coupling of the Red Sea sea-level

signal with Asian monsoon records (Grant et al., 2014). By contrast, past sea-level reconstructions derived from oxygene isotope analysis of speleothems (Bard et al., 2002; Dutton et al., 2009) would indicate that sea level during the MIS 7 stage maintained continuously below psl, at a depth of around −18 m. Similar results, suggesting that paleo-sea level during the penultimate interglacial stage has fluctuated between 10 m and 17 m below psl, were gained from the analysis of inclined reef cores at Moruroa (Camoin et al., 2001). During the MIS 9 stage, sea level is inferred to have peaked at levels close to present (Siddall et al., 2006; Rohling et al., 2009; Murray-Wallace and Woodroffe, 2014).

5.7 Comparison with the composition of coral communities I in some other Tuamotu and Pacific atolls

Compositional and distributional patterns of corals along outer-reef slopes from atolls, are known to be controlled, not only by bathymetry and water agitation, but also by reef orientation, and slope gradient (Wells, 1956; Kühlmann, 1982; Bouchon, 1983; Faure and Laboute, 1984; Laboute, 1985; Kühlmann and Chevalier, 1986; Maragos, 1994). At Takapoto, as observed in both windward and leeward sides, *Pocillopora* remains dominating within the upper −10 m to −15 m along gently sloping spurs (TL1), and terraces TL2, while *Porites* achieves prominence from −15 m to −30 m, along steeper to sub-vertical

slopes (Bouchon, 1983; Kühlmann and Chevalier, 1986). Similar trends were reported from the nearby Tikehau Atoll (Faure and Laboute, 1984).

Coral cover rates from other Pacific atolls are poorly documented (Wells, 1954; Maragos, 1994). The only detailed, quantitative coral censuses of seaward outer margins were carried out on Mili and Rongelap Atolls (Marshall Islands, central Pacific) at different depths between −5 m and −20 m (Pinca et al., 2006). *Porites* is by far the most abundant genus (14–62 %) in both leeward and windward sites. Surprisingly, robust branching *Pocillopora*, 12 % to up to 20 % in cover rates, are restricted to lagoons, apparently missing from open-sea environments. By contrast, on some other Marshall Islands (Bikini, northern atolls), as on Takapoto, *Pocillopora* species are amongst the most common outer-reef dwellers, especially in the upper fore-reef parts (Wells, 1954; Maragos, 1994). These observations indicate there can have marked, within-region to inter-regional differences in coral composition, maybe due to. competitive interactions between coral groups (Lenihan et al., 2011). Anyway, in the study areas, coral growths contribute intensively to shaping of upper fore-reef slopes to depths greater than 40 m.

The present study confirmed the reliability of robust-branching *Pocillopora verrucosa* as a relative sea-level marker as previously demonstrated in some Indo-Pacific reef sites

(Montaggioni and Faure, 1997; Montaggioni et al., 1997; Cabioch et al., 1999; Camoin et al., 2001). Composite *P. verrucosa*-dominated frameworks appeared to be restricted to the 0–10 m depth range.

6 Conclusions

Detailed geomorphological analysis of satellite-based bathymetric profiles obtained from fore-reef zones all around Takapoto Atoll, using spaceborne imagery, together with direct underwater observations of fine-scale geomorphic features and coral community composition, allows the following conclusions to be drawn.

1. Six distinct fore-reef sectors were delineated based on seaward extension to the detected slope depths and mean slope gradients. The lowest gradient (< 30°–35°) and most extended (close to 200 m) sectors are situated at the northern atoll end and along a short portion of the mid-south-eastern side. It exhibits wide terraces and low steps. The north-eastern sector displays highest gradient (68° on average) and narrowest (90 m) slopes and narrow terraces. The remaining eastern and north-western sectors, together with south-western and southern ends have steep slopes (52° to 57° on average), extending seawards over 90 m to 100 m on average, with narrow terraces and high steps.

2. Among the described geomorphic features, of specific interest are terraces, outer-reef crest-like reliefs, pinnacles, steps and drop-offs, scars and trenches to reconstruct the development history of fore-reef zones.

Seven levels of submerged terraces were identified at depths averaging −5 m, −10 m, −15 m, −20 m, −24 m, −30.5 m, and −38 m respectively. These range from about 45 m to 2 m in width. The shallowest terrace level refers to the present-day surfaces of spurs. In lack of any radiometric dating, the deeper terrace levels were postulated to be remnants of a series of Pleistocene reef tracts, severely altered by sub-aerial erosion during periods of emergence, and finally overlapped by coral veneers during the post-glacial marine transgression, from about 9.5 ky to present. This scenario is in great part based on comparisons with subsurface reef chronostratigraphy from several Pacific atolls. The rates of sub-aerial erosion and linear subsidence were estimated at $0.12\ \mathrm{mm} \cdot \mathrm{y}^{-1}$ and $0.047\ \mathrm{mm} \cdot \mathrm{y}^{-1}$ respectively from comparisons with calculated surface lowering of Pacific atolls and usually accepted sea-level position at 125 ka. After depth correction of ground lowering and of subsidence effects, the interglacial high sea-stands during which each reef tract has formed and the position of the corresponding sea level were

tentatively defined. The 10-m, 14.5m, 20-m, 24-m and 30.5-m terraces were expected to relate to the MIS 5e, 7a, 7c, 7e and 9e respectively, despite substantial uncertainties on elevation estimates.

Outer reef crest-like features, less than 2 m high, occur frequently at the seaward edge of terraces. Similarly, steep-walled pinnacles are commun at different places and depths on terraces and slopes. Both were considered to be remains of coralgal buildups, unable to compensate with the post-glacial sea-level rise.

Steps and drop-offs, a few metres to more than 15 m high, are presumably remains of the foreslopes of pre-existing reef tracts or preserved scars of partially collapsed fore-reef slopes. Trenchs cutting the fore-reef zone were found locally and represent detachment fissures. The faces of the western and eastern fore-reef slopes are aligned in south-west to north-east direction, consistent with the main axis orientation of the atoll. This direction is that of atoll-bearing, submarine volcanic ridges discovered in the north-western part of the Tuamotu plateau, generated from and shaped by underlying lithospheric fractures.

3. Compositional and distributional patterns of coral populations at the study site are in agreement with previous investigations in the Tuamotu atolls. Robust

branching *Pocillopora* forms appear to be the main builders on the uppermost, gently dipping parts of fore-reef zones, to the depth of about 10 m. This explains why this species is regarded as diagnostic in terms of paleo-bathymetry reconstruction. Pocilloporids are replaced by sub-massive to plate-shaped *Porites*, profusely growing from −15 m to −35 m deep at least. Concerning biogeographic distribution of corals across the central Pacific, there are noticeable differences between the Marshall and Tuamotu islands, probably controlled mainly by local ecological constraints. However, along upper fore-reef zones, coral growths appear to play a key role in controlling superficial morphogenesis.

Acknowledgments

The present work was supported by the French national research agency (CNRS) under the STORISK research project (N° ANR-15-CE03-0003) coordinated by Virginie Duvat. Field work has benefited from logistical support and help from the research station of the Office of Marine Resources in Takapoto, Gaby Maiti Haumani. Bathymetric, satellite and echo-sounder-based records were provided by AC and treated by DJ. Data on the composition and distribution of coral communities were provided by GS and MT, and exploited by YC. LM, the corresponding author, analysed

and interpreted the data, and wrote the manuscript with imput from the co-authors. Figures were conceived by LM and BM-G.

References

Abbey, E., Webster, J.M., Beaman, R.J., 2011. Geomorphology of submerged reefs on the shelf edge of the Great Barrier Reef: the influence of oscillating Pleistocene sea-levels. Mar. Geol. 288, 61–78.

Adam, C., Yoshida, M., Suetsugu, D., Fukao, Y., Cadio, C., 2014. Geodynamic modeling of the South Pacific superswell. Phys. Earth Planet. Interiors 229, 24–39.

Adey, W. H., 1978. Algal ridges of the Caribbean Sea and West Indies. Phycologia 17, 361–367.

Adey, W.H., 1986. Coralline algae as indicators of sea level. In: Van de Plassche, O. (ed). Sea-level Research: A manual for the Collection and Evaluation of Data, Springer, Dordretch, p.229–280.

Andréfoüet, S., Ardhuin, F., Queffeulou, P., Le Gendre, R., 2012. Island shadow effect and the wave climate of the Western Tuamotu Archipelago (French Polynesia) inferred from altimetry and numerical model data. Mar. Pollut. Bull. 65, 415–424.

Arai, K., Matsuda, H., Sasaki, K., Machiyama, H., Yamaguchi, T., Inoue, T., Sato, T., Takayanagi, H., Iryu, Y., 2016. A newly discovered submerged reef on the Miyako-Sone

platform, Ryukyu Island Arc, northwestern Pacific. Mar. Geol. 373, 49–54.

Austermann, J., Mitrovica, J.X., Huybers, P., Rovere, A., 2017. Detection of a dynamic topography signal in last interglacial sea-level records. Sci. Adv. 3, e 1700457.

Bard, E., Hamelin, B., Arnold, M., Montaggioni, L.F., Cabioch, G., Faure, G., Rougerie, F., 1996. Deglacial sea-level record from Tahiti corals and the timing of global meltwater discharge. Nature 382, 241–244.

Bard, E., Antonioli, F., Silenzi, S., 2002. Sea-level during the penultimate interglacial period based on a submerged stalagmite from Argentarola Cave (Italy). Earth Planet. Sci. Lett. 196, 135–146.

Bard, E., Hamelin, B., Delanghe-Sabatier, D., 2010. Deglacial meltwater pulse 1B and Younger Dryas sea-levels revisited with boreholes at Tahiti. Science 327, 1235–1237.

Beaman, R.J., Webster, J.M., Wust, R.A.J., 2008. New evidence for drowned shelf edge reefs in the Great Barrier Reef, Australia. Mar. Geol. 247, 17–34.

Blanchon, P., Jones, B., Ford, D.C., 2002. Discovery of submerged relic reef and shoreline off Grand Cayman: further evidence for an early Holocene jump in sea level. Sedim. Geol. 147, 253–270.

Bouchon, C., 1983. Les peuplements de scléractiniaires de l'atoll de Takapoto (Polynésie Française). J. Soc. Océanistes 39, 35–42.

Buigues, D., 1997. Geology and hydrology of Mururoa and Fangataufa, French Polynesia. In: Vacher, H.L., Quinn, T.M. (eds). Geology and Hydrology of Carbonate Islands, Elsevier, Amsterdam, Develop. Sediment. 54, 433–452

Cabioch, G., Montaggioni, L.F., Faure, G., Ribaud-Laurenti, A. 1999. Reef coralgal assemblages as recorders of paleobathymetry and sea level changes in the Indo-Pacific province. Quat. Sci. Rev. 18, 1681–1695.

Cabioch, G., Montaggioni, L.F., Norbert, F., Seard, C., Sallé, E., Payri, C., Pelletier, B., Paterne, M., 2008. Successive reef depositional events along the Marquesas foreslopes (French Polynesia) since 26 ka. Mar. Geol. 254, 18–34.

Camoin, G.F., Ebren, Ph., Eisenhauer, A., Bard, E., Faure, G., 2001. A 300,000-yr coral reef record of sea-level changes, Mururoa Atoll (Tuamotu Archipelago, French Polynesia). Palaeogeogr. Palaeoclimatol. Palaeoecol. 175, 325–341.

Camoin, G.F., Seard, C., Deschamps P., Webster, J.M., Abbey, E., Braga, J.C., Iryu, Y., Durand, N., Bard, E., Hamelin, B., Yokoyama, Y., Thomas, A.L. Henderson, G.M., Dussoulliez, Ph., 2012. Reef response to sea-level and environmental changes during the last deglaciation: Integrated Ocean Drilling Program Expedition 310, Tahiti Sea Level. Geology 40, 643–646.

Camoin, G. F., Webster, J.M., 2015. Coral reef response to Quaternary sea-level and environmental changes: state-of-the art. Sedimentology 61, 401–428.

Chevalier, J.-P., Salvat, B., 1976. Eude géomorphologique de l'atoll fermé de Taiaro. Cah. Pac. 19, 169–201.

Chevalier, J.-P., Denizot, M., 1979. Les organismes constructeurs de l'atoll de Takapoto. J. Soc. Océan. 35, 30–34.

Chevalier, J.-P., Denizot, M., Mougin, J.L., Plessis, Y., Salvat, B., 1968. Etude géomorphologique et bionomique de l'atoll de Mururoa (Tuamotu). Cah. Pacifique 12, 1–144.

Chevalier, J.-P., Denizot, M., Ricard, M., Salvat, B., Sournia, A., Vasseur, P., 1979. Géomorphologie de l'atoll de Takapoto. J. Soc. Océanistes 35, 9–18.

Collin, A., Duvat, V., Pillet, V., Salvat, B., James, D., 2018. Understanding interactions between shoreline changes and reef slope morphometry on Takapoto Atoll (French Polynesia). J. Coast.Res. SI 496–500.

Dullo, W.Ch., 2005. Coral growth and reef growth: a brief review. Facies 51, 33–48.

Dullo, W.Ch., Camoin, G.F., Blomeier, D., Colonna, M., Eisenhauer, A., Faure, G., Casanova, J., Thomassin, B.A., 1998. Morphology and sediments of the fore-slopes of Mayotte, Comoro Islands: direct observations from a submersible. In: Camoin, G.F., Davies, P.J. (eds). Reefs and Carbonate Platforms in the Pacific and Indian Oceans, Intern. Assoc. Sedimentologists, Spec. Publ. 27, 217–238.

Duncan, R. A., Clague, D. A., 1985. Pacific plate motion recorded by linear volcanic chains. In: Nairn, A.E.A. et al. (eds). The Ocean Basins and Margins, 7A, The Pacific Ocean, Plenum, New York, pp. 89–121.

Dutton, A., Bard, E., Antonioli, F., Esat, T.M., Lambeck, K., McCulloch, M.T., 2009. Phasing and amplitude of sea-

level and cimate change during the penultimate interglacial. Nature Geosciences DOI: 10.1038/ngeo470

Dutton, A., Lambeck, K., 2012. Ice volume and sea level during the last interglacial. Science 337, 216–219.

Emery, K.O., Tracey, J.I.,Jr., Ladd, H.S., 1954. Geology of Bikini and nearby atolls: U.S. Geol. Surv. Prof. Paper 260 A, 1–265 pp.

Faichney, I.D.E., Webster, J.M., Clague, D., Kelley, Ch., Appelgate, B., Moore, J.G., 2009. The morphology and distribution of submerged reefs. In the Maui-Nui Complex, Hawaii: new insights into their evolution since the early Pleistocene. Mar. Geol. 265, 130–145.

Faichney, I.D.E., Webster, J.M., Clague, D.A., Paduan, J.B., Fullagar, P.D., 2010. Unravaling the tilting history of the submerged reefs surrounding Oahu and the Maui_Nui Complex, Hawaii. Geochem. Geophys. Geosyst. 11, Q07002, DOI: 10.1029/2010GC003044

Fairbanks, R.G., 1979. A 17,000-year glacio-eustatic sea level record: influence of glacial melting rates on the Younger Dryas event and deep-ocean circulation. Nature 342, 637–642.

Fairbridge, R.W., 1950. Landslide patterns on oceanic volcanoes and atolls. The Geogr. J. 115, 84–88.

Faure, G., Laboute, P., 1984. Formations récifales 1: Définitions des unités récifales et distribution des principaux peuplements de scléractiniaires. In: L'atoll de Tikehau (Archipel des Tuamotu, Polynésie française), Premiers

Résultats. Notes et Doc. Océanogr., Office Rech. Sci. Techn. Outre-Mer 22, 108–136.

Gischler, E., Hudson, J.H., Pisera, A., 2008. Late Quaternary reef growth and sea level in the Maldives (Indian Ocean). Mar. Geol. 250, 104–113.

Gischler, E., Hudson, J.H., 2019. Holocene tropical reef accretion and lagoon sedimentation: a quantitative approach to the influence of sea-level rise, climate and subsidence (Belize, Maldives, French Polynesia). The Depositional Record 5: https://doi.org/10.1002/dep2.62.

Grant, K.M., Rohling, E.J., Ramsey, C.B., Cheng, H., Edwards, R.L., Florindo, F., Heslope, D., Marra, F., Roberts, A.P., Tamisiea, M.E., Williams, F., 2014. Sea-level variability over five glacial cycles. Nature Comm. 5:5076. DOI: 10.1038/ncomms6076.

Gray, S.C, Hein, J.R., Hausmann, R., Radtke, U., 1992. Geochronology and subsurface stratigraphy of Pukapuka and Rakahanga atolls, Cook Islands: late Quaternary reef growth and sea level history. Palaeogeogr. Palaeoclim. Palaeoecol 91, 377–393.

Green, A.N., Cooper, J.A.G., Salzmann, L., 2014. Geomorphic and stratigraphic signals of postglacial meltwater pulses on continental shelves. Geology 42, 151–154.

Guozhong, W., Bingquan, L., Songqing, Q., 1990. Sedimentary characteristics of coral reefs in the northern part of the South China Sea. Atoll Res. Bull. 346, 1–21.

Harmelin-Vivien, M.L., Laboute, P., 1986. Catastrophic impact of hurricanes on atoll outer reef slopes in the Tuamotu (French Polynesia). Coral Reefs 5, 55–62.

Hearty, P.J., Kindler, P., 1995. Sea-level high stand chronology from stable carbonate platforms (Bermuda and Bahamas). J.Coast. Res.11, 675–689.

Hopley, D., 1982. The Geomorphology of the Great Barrier Reef: Quaternary Development of Coral Reefs. Wiley-Intetscience, New-York, 453 pp.

Hopley, D., Smithers, S.G., Parnell, K.E., 2007. The Geomorphology of the Great Barrier Reef: Development, Diversity and Change. Cambridge Univ. Press, Cambridge, UK, 532 pp.

Hubbard, D. K., Dullo, W.Ch., 2016. The Changing Face of Reef Building. In: Hubbard, D. K., Rogers, C. S., Lipps, J. H., Stanley, G. D (eds). Coral Reefs at the Crossroads. Coral Reefs of the World, 6. Springer, Dordrecht, pp. 127–153.

Ito, G., McNutt, M., Gibson, R.L., 1995. Crustal structure of the Tuamotu Plateau, 15°S, and implications for its origin. J. Geophys. Res. 100, 8097–8114.

Jackson, E.D., Schlanger, S.O., 1976. Regional syntheses, Line Islands chain, Tuamotu Island chain and Manihiki Plateau, central Pacific Ocean. Init Repts, DSDP 33, 915–927.

James, N.P., Ginsburg, R.N., 1979. The seaward margin of Belize Barrier and Atoll Reefs. Intern. Assoc. Sedimentologists, Spec. Publ. 3, Blackwell, Oxford, 191 pp.

Jian, L., Zhizheng, Y., Chunrui, H., Xinbo, L., Gaosheng, Q., 1997. Meteoric diagenesis in Pleistocene reef limestones of Xisha Islands, China. J.Asian Earth Sci. 15, 465–476.

Jordahl, K., Caress, D., McNutt, M., Bonneville, A., 2004. Sea-floor topography and morphology of the Superswell Region. In: Hekinian, R., Stoffers, P., Cheminée, J.-L. (eds). Oceanic Hotspots: Intraplate submarine Magmatism and Tectonism, Springer, Berlin, pp. 9–28.

Keating, B.H., 1987. Structural failure and drowning of Johnston Atoll, central Pacific Basin. In: Keating, B.H., Fryer, P., Batiza, R., Boehlert, G.W. (eds). Seamounts, Islands and Atolls. American Geophys. Union, Washington, D.C., Geophys. Monograph Ser. 43, pp. 40–60.

Keating, B.H., 1998. Side-scan sonar images of submarine landslides on the flanks of atolls and guyots. Mar. Geodesy 21, 129–145.

Keating, B.H., McGuire, J.M., 2000. Island failures and associated tsunami hazards. Pure Appl. Geophys. 157, 899–955.

Khanna, P., Droxler, A., Nittrouer, J.A., Tunnell, J., Shirley, Th. C., 2017. Coralgal reef morphology records punctuated sea-level rise during the last deglaciation. Nature Comm., 8: 1046. DOI/ 10.1038/s41467-017-00966-x.

Kopp, R.E., Simmons, F.J., Mitrovica, J.X., Maloof, A.C., Oppenheimer, M., 2009. Probablistic assessment of sea

level during the last interglacial stage. Nature 462, 863–867.

Korenaga, T., Korenaga, J., 2008. Subsidence of normal oceanic lithosphere, apparent thermal expansivity, and sea floor flattening. Earth Planet. Sci. Lett. 268, 41–51.

Kühlmann, H.H., 1982. Zusammensetzung und ökologie von Tiefwasser-Korallenassoziationen. Wissenschaftliche Zeitschrift der Humbolt-Universität zu Berlin. Math-Nat. R, 31, 233–244.

Kühlmann, H.H., Chevalier, J.P., 1986. The corals (Scleractinians and Hydrocorals) of the Takapoto Atoll, Tuamotu Islands: ecological aspects. Mar. Ecol. 7, 75–104.

Laboute, P., 1985. Evaluation des dégats causés par les passages des cyclones de 1982–1983 en Polynésie Française sur les pentes externes des atolls de Tikehau et de Takapoto (Archipel des Tuamotu). Proc. Fifth Internat. Coral Reef Congr. 3, 323–329.

Ladd, H.S., Tracey, Jr., I.J., Gross, M.G., 1970. Deep drilling on Midway Atoll. US Geol. Surv. Prof. Papers 680-A, A1–A22.

Larrue, S., Chiron, Th., 2010. Les îles de Polynésie Française face à l'aléa cyclonique. Vertigo 10. https://doi.org/10.4000/vertigo.10558.

Lea, D.W., Martin, P.A., Pak, D.K., Spero, H.J., 2002. Reconstructing a 350 history of sea level using planktonic Mg/Ca and oxygen isotope record from a Cocos Ridge core. Quat. Sci. Rev. 21, 283–293.

Lenihan, H.S., Holbrook, S.J., Schmitt, R.J., Brooks, A.J., 2011. Influence of corallivory, competition, and habitat structure on coral community shifts. Ecology 92, 1959–1971. doi.org/10.1890/11-0108.1

Li., W.-X., Lundberg, J., Dickin, A.P., Ford, D.C., Schwarcz, H.P., McNutt, R., Williams, D., 1989. High precision mass spectrometric uranium-series dating of cave deposits and implications for paleoclimate studies. Nature 339, 564–536.

Lighty, R.G., Macintyre, I. G., Stuckenrath, R., 1978. Submerged early Holocene barrier reef, south-east Florida shelf. Nature 276, 59–60.

Lincoln, J.M., Schlanger, S.O., 1991. Atoll stratigraphy as record of sea level changes: problems and prospects. J. Geophys. Res. 96, 6727–6752.

Linklater, M., Brooke, B. P., Hamylton, S. M., Nichol, S. L., Woodroffe, C. D., 2015. Submerged fossil reefs discovered beyond the limit of modern reef growth in the Pacific Ocean. Geomorphology 246, 579–588.

Lundberg, J., Ford, D.C., 1994. Late Pleistocene sea level change in the Bahamas from mass spectrometric U-series dating of submerged speleothem. Quat. Sci. Rev. 13, 1–14.

Mahoney, J.J., 1987. An Isotopic Survey of Pacific Oceanic Plateaus: Implications for their Nature and Origin. In: Keating, B.H., Fryer, P., Batiza, R., Boehlert, G.W. (eds) Seamounts, Islands and Atolls. American Geophys. Union,

Washington, D.C., Geophys. Monogr. Ser. 43, pp. 207–220.

Maragos, J.E., 1994. Description of reefs and corals for the 1988 protected area survey of the northern Marshall Islands. Atoll Res. Bull. 419, 88 pp.

Marshall, J.F., Jacobsen, G., 1985. Holocene growth of a mid-Pacific atoll: Tarawa, Kiribati. Coral Reefs 4, 11–14.

McNutt, M., Fischer, K.M., 1987. The South Pacific Superswell. In: Keating, B.H., Fryer, P., Batiza, R., Boehlert, G.W. (eds). Seamounts, Islands and Atolls. America Geophys. Union, Washington, D.C., Geophys. Monograph Ser. 43, pp. 25–34.

McNutt, M., 1998. Superswells, Rev. Geophys. 36, 211– 244.

Menard, H.W., 1969. Elevation and subsidence of oceanic crust. Earth Planet. Sci. Lett. 6, 275–284.

Montaggioni, L.F., 1985. Makatea Island. Proc. Fifth Int. Coral Reef Congress, Tahiti, 1, 103–158.

Montaggioni, L.F., 2005. History of Indo-Pacific coral reef systems since the last deglaciation: development patterns and controlling factors. Earth Sci. Rev. 71, 1–75.

Montaggioni, L.F., Gabrié, C., Naim, O., Payri, C., Richard, G., Salvat, B., 1987. The seaward margin of Makatea, an uplifted carbonate island (Tuamotu, central Pacific). Atoll. Res. Bull. 299, 1–18.

Montaggioni, L.F., Faure, G., 1997. Response of coral reef communities to sea level rise: A Holocene model from Mauritius (Western Indian Ocean). Sedimentology 44, 1053–1070.

Montaggioni, L.F., Cabioch, G., Camoin, G.F., Bard, E., Ribaud-Laurenti, A., Faure, G., Déjardin, P., Récy, J., 1997. Continuous record of reef growth over the past 14 ky on the mid-Pacific island of Tahiti. Geology 25, 555–558.

Montaggioni L.F., Braithwaite, C.J.R., 2009. Quaternary Coral Reef Systems: Development processes and controlling factors. Developments in Marine Geology 5. Elsevier, Amsterdam, 532 pp.

Montaggioni, L.F., Borgomano, J., Fournier, F., Granjeon, D. 2015. Quaternary atoll development: New insights from the two-dimensionam stratigraphic forward modeling of Mururoa Island (Central Pacific). Sedimentology 62, 466–500.

Montaggioni, L.F., Salvat, B., Aubanel, A., Eisenhauer, A., Martin-Garin, B., 2018. The mode and timing of windward reef-island accretion in relation with Holocene sea-level change: a case study from Takapoto Atoll, French Polynesia. Geomorphology 318, 320–335.

Muhs, D.R., 2002. Evidence for the timing and duration of the last interglacial period from the high-precision uranium-series ages of corals on tectonically stable coastlines. Quat. Res. 58, 36–40.

Müller, R.D., Sdrolias, M., Gaina, C., Roest, W.R., 2008. Age, spreading rates, and spreading assymmetry of the world's ocean crust. Geochem. Geophys. Geosyst. 9, Q04006, doi:10.1029/2007GC001743

Murray-Wallace, C.V., Woodroffe, C.D., 2014. Quaternary sea-level changes. Cambrige Univ. Press, Cambridge, UK, 484 pp.

Neumann, A.C., Macintyre, I., 1985. Reef response of sea level rise: keep-up, catch-up or give-up. Proc. Fifth Int. Coral Reef Congr. 3, 105–110.

Okal, E.A., Cazenave, J., 1985. A model for the plate tectonic evolution of the east-central Pacific based on Seasat investigations. Earth Planet Sc Lett 72, 99–116.

Patriat, M., Kingelhoefer, F., Aslanian, D., Contrucci, I., Gutscher, M.-A., Talandier, J., Avedik, F., Francheteau, J., Weigel, W., 2002. Deep crustal structure of the Tuamotu plateau and Tahiti (French Polynesia) based on seismic refraction data. Geophys. Res. Lett. 29, 388–391.

Paulay, G., McEdward, L.R., 1990. A simulation model of reef island morphology: the effects of sea level fluctuations, growth, subsidence and erosion. Coral Reefs 9, 51–62.

Phinney, J.T., Hoegh-Guldberg, O., Kleypas, J., Skirving, W. (eds), 2013. Coral Reefs and Climate Change: Science and Management. American Gephys. Union, Coast. Estuarines Stud., Wiley, New-York, 61, 244 pp.

Pinca, S., Beger, M., Muller, B., Reeves, E., White, M., 2006. Community analysis of reef habitats in the Marshall Islands. Proc. Tenth Int. Coral Reef Symp. Okinawa, Japan, 300–305.

Poppenga, S.K., Palaseanu-Lovejoy, M., Gesch, D.B., Danielson, J.J, Tyler, D.J., 2018. Evaluating the potential for near-shore bathymetry on the Majuro Atoll, Republic of the Marshall Islands, using Landsat 8 and WorldView-3 Imagery. US Geol. Surv. Scientific Investigations Report 2018–5024, 14 pp.

Poupardin, A., Henrich, Ph., Frère, A., Imbert, D., Hébert, H., Flouzat, M., 2017. The 1979 submarine landsline-generated tsunami in Mururoa, French Polynesia. Pure Appl. Geophys. 174, 3293–3311.

Puga-Bernabéu, A., Beaman, R.J., Webster, J.M., Thomas, A.L., Jacobsen, G., 2017. Gloria Knolls slide: a prominent submarine landslide complex on the Great Barrier Reef margin of north-eastern Australia. Mar. Geol. 385, 68–83.

Purdy, E.G., Winterer, E.L., 2001. Origin of atoll lagoons. American Geol. Soc. Bull. 113, 837–854.

Quinn, T.M., 1991. The history of post-Miocene sea level change: inferences from stratigraphic modeling of Enewatok Atoll. J. Geophys. Res. 96, 6713–6725.

Ristvet, B.L., Couch, Jr., R.F., Tremba, E.L., 1980. Late Cenozoic solution unconformities at Enewetak Atoll. Geol. Soc. America Bull. Abstracts Programs 12, 510.

Riyaz, M., Park, K.H., 2008. Reef slope failure in the north-eastern corner of Malé, Maldives. Proc. Eleventh Coral Reef Symp. Fort Lauderdale, Florida, session 1, 31–33.

Rohling, E.J., Grant, K., Bolshaw, M., Roberts, A.P., Siddall, M., Hembelen, Ch., Kucera, M., 2009. Antarctic temperature and global sea level closely coupled over the past five glacial cycles. Nat. Geosci. 2, 500–504.

Rovere, A., Khanna, P., Bianchi, C.N, Droxler, A.W., 2018. Submerged reef terraces in the Maldivian Archipelao (Indian Ocean). Geomorphology 317, 218–232.

Rufin-Soler, C., Mörner, N.-A., Laborel, J., Collina-Girard, J., 2013. Submarine morphology in the Maldives and Holocene sea-level rise. Mar. Biodivers. 45, 599–600.

Salvat, B., 1981. Geomorphology and marine ecology of the Takapoto Atoll. Proc. Fourth Intern. Coral Reef Symp., Univ.Philippines, Manila, 1, 503–509.

Salvat, B., Richard, G., 1985. Takapoto Atoll, Tuamotu Archipelago. Proc. Intern. Coral Reef Congr. 1, pp. 323–378.

Sanborn, K.L., Webster, J.M., Yokoyama, Y., Dutton, A., Braga, J.C., Clague, D.A., Paduan, J.B., Wagner, D., Rooney, J.J., Hansen, J.R., 2010. Evidence of Hawaiian coral reef drowning in response to meltwater pulse 1A. Quat. Sci. Rev. 175, 60–72.

Schellmann, G., Radtke, U., 2004. A revised morpho- and chronostratigraphy of the late and middle Pleistocene coral reef terraces on southern Barbados (West Indies). Earth Sci. Rev. 64, 157–187.

Schlanger, S. O., Garcia, M. O., Keating, B. H., Naughton, J. J., Sager, W. W., Haggerty, J. A., Philpotts, J. A., Duncan, R. A., 1984. Geology and Geochronology of the Line Islands, J. Geophys. Res. 89, 11261– 11272.

Schlanger, S.O., Campbell, J.F. Jackson, M.W., 1987. Post-Eocene subsidence of the Marshall Islands recorded by drowned atolls on Harrie and Sylvania guyots. In: Keating, B.H., Fryer, P., Batiza, R., Boehlert, G.W. (eds) Seamounts, Islands and Atolls Geophys. Monogr. American Geophys. Union 43, 165–174.

Seard, C., Borgomano, J., Granjeon, D., Camoin, G.F., 2013. Impact of environmental parameters on coral reef development and drowning: forward modelling of the last deglacial reefs from Tahiti (French Polynesia; IODP Expedition ♯ 310. Sedimentology 60, 1357–1388.

Siddall, M., Rohling, E.J., Almogi-Labin, A., Hemleben, Ch., Meischner, D., Schmelzer, I., Smeed, D.A., 2003. Sea-level fluctuations during the last glacial cycle. Nature 423, 853–858.

Siddall, M., Chappell, J., Potter, E.K., 2006. Eustatic sea level during past interglacials. In: Sirocko, F., Litt, T., Claussen, M., Sanchez-Goni, M.F. (eds) The climate of past interglacials, Elsevier, Amsterdam, p. 75–92.

Siddall, M., Chappell, J., Potter, E.K., 2007. Eustatic sea-level during past interglacials. Dev. Quat. Sci. 7, 75–92.

Sladen, A., Hébert, H., Schindelé, F., Reymond, D., 2007. Evaluation of far-field tsunami hazard in French Polynesia based on historical and numerical simulations. Nat. Hazards Earth Syst. Sci. 7, 195–206.

Smith, R., Young, S., Biribo, N., 1994. Bathymetric, seismic and alternative sand and gravel resource surveys, Tarawa Atoll, Kiribati. SOPAC Preliminary Report 72, 14 pp.

Stumpf, R., Holderied K., Sinclair, M., 2003. Determination of water depth with high-resolution satellite imagery over variable bottom types. Limnol. Oceanogr. 48, 547–556.

Szabo, B.J., Tracey, Jr., J.I., Goter, E.R., 1985. Age of subsurface stratigraphic intervals in the Quaternary of Enewetak Atoll, Marshall Islands. Quat. Res. 23, 54–61.

Terry, J.P., Goff, J., 2012. One hundred and thirty years since Darwin: reshaping the theory of atoll formation. The Holocene 23, 615–619.

Terry, J.P., Goff, J., 2017. Comment on 'Late Cenozoic sea level and the rise of modern rimmed atolls' by Toomey et al. (2016), Palaeogeogr. Palaeoclim. Palaeoecol. 451: 73–83; Palaeogeogr. Palaeoclim. Palaeoecol. 469, 156–158.

Thompson, W.G., Goldstein, S.L., 2005. Open-system coral ages reveal persistent suborbital sea-level cycles. Science 308, 401–404.

Thompson, W.G, Spiegelman, M.W., Goldstein, S.L., Speed, R.P., 2003. An open-system model for U-series age determinations of fossil corals. Earth Planet. Sci. Lett. 210, 365–381.

Tracey, Jr., J.I., Ladd, H.S., 1974. Quaternary history of Eniwetok and Bikini atolls, Marshall Islands. Proc. Second Intern. Coral Reef Symp., Great Barrier Reef Committee, Brisbane, 2, 537–550.

Webster, J.M., et al., 2004a. Drowning of the −150 m reef off Hawaii: a casualty of global meltwater pulse 1A? Geology 32, 249–252.

Webster, J.M., Wallace, L., Silver, E., Applegate, B., Potts, D., Riker-Coleman, K., Gallup, C., 2004b. Drowned carbonate platforms in the Huon Gulf, Papua New Guinea. Geochem. Geophys. Geosyst. 5, Q11008, doi:10.1029/2004GC000726.

Webster, J.M., Clague, D.A., Braga, J.C., Spalding, H., Renema, W., Kelley, Ch., Applegate, B., Smith, J.R., Paull, C.K.,

Moore, J.G., Potts, D., 2006. Drowned coralline algal dominated deposits off Lanai, Hawaii; carbonate accretion and vertical tectonics over the last 30 ka. Mar. Geol. 225, 223.

Webster, J.M., Braga, J.C., Clague, D.A., Gallup, C., Hein, J.R., Potts, D.C., Renema, W., Riding, R., Riker-Coleman, K., Silver, E., Wallace, L.M., 2009. Coral reef evolution on rapidly subsiding margins. Global Planet. Change 66, 129–148.

Webster, J.M., George, N.P.G., Beaman, R.J., Hill, J., Puga-Bernabéu, A., Hinestrosa, G., Abbey, E.A., Daniell, J., 2016. Submarine landslides on the Great Barrier Reef shelf edge and upper slope: a mechanism for generating tsunamis on the north-east Australian coast? Mar. Geol. 371, 120–129.

Webster, J.M., Braga, J.C., Humblet, M., Potts, D.C. Iryu, Y., Yokoyama, Y., Fujita, K., Bourillot, R., Esat, T.M., Fallon S., Thompson, W.G., Thomas, A.L., Kan, H., McGregor, H.V., Hinestrosa, G., Obrochta, S.P., Lougheed, B.C., 2018. Response of the Great Barrier Reef to sea-level and environmental changes over the past 30,000 years. Nat. Geosci. 11, 426–432.

Wells, J.W., 1954. Recent corals of the Marshall Islands. U.S. Geol. Surv. Prof. Paper. 260–1: 385–486.

Winterer, E.L., 1976. Bathymetry and and regional tectonic setting of the Line Islands Chain. Initial Reports, DSDP 33, 25, 731–747.

Woodroffe, C.D., Webster, J.M., 2014. Coral reefs and sea-level change. Mar. Geol. 352, 248–267.

Wong, F.L., Hein, J.R., Mosier, D.L., 1999. Gridded bathymetric data for the Republic of the Marshall Islands. USGS Miscellaneous Field Stud. Map, US Geol. Surv. MF 2324.

7 Table captions

Table 1. Geomorphic features identified along the fore-reef slopes of Takapoto Atoll.

Table 2. Coral cover rate at different depths along fore-reef slopes (−5 m, −10 m, −15 m, −20 m, −25 m, and −30 m), south end, Fakatopatere area, Takapoto Atoll.

Table 3. Depth distribution of terrace levels (TL3 to TL6) identified from fore-reef slopes at Takapoto Atoll, and interpreted in terms of paleo-sea level positions.
The following parameters are given: time duration (ky) of MIS substage; duration (ky) during which terraces were exposed to sub-aerial erosion; time at which terraces were re-fooded by sea-level rise (ka); amplitude of subsidence and ground lowering (metres); resulting deepening (metres) of terraces; interpretative eustatic paleo-high sea stands.

8 Figure captions

Fig. 1. (a) Location map of Takapoto Atoll in the Tuamotu Archipelago (French Polynesia, Central Pacific). (b) Bathymetric and structural map of the northern area of the Tuamotu Plateau. Are specifically indicated the location of atolls (Manihi, Takaroa, Ahe, Raroia, Takume) whose major axis of elongation is oriented south-west–north-east, consistent with that of Takapoto and a number of nearby submarine

volcanic ridges (SVR). Background map from Google Earth Pro

Fig. 2. Google Earth Pro aerial maps of Takapoto Atoll. (a) Location of water-depth sounding tracks along the eastern outer margin of the atoll and landslide-related scars. (b) Location of satellite-derived bathymetric profiles (T1 to T41) around the atoll fore-reef slope, running from the modern outer reef crest to the deepest detected toe. Colors refer to profile length.

Fig. 3. Virtual bathymetric profile showing the different geomorphic features identified along the fore-reef slopes at Takapoto.

Fig. 4. Plots of bathymetric profiles from the six fore-reef sectors delineated around the atoll, on the basis of profile length and gradient. See figure 2b for location of profiles.

Fig. 5. Selected bathymetric profiles from each delineated fore-reef sector showing local geomorphic attributes. See figure 2b for location of profiles.

Fig. 6. 3-D reconstruction of a portion of the WSW side at Takapoto Atoll, based on satellite imagery surveys.The image portion is lying between the profiles T26 and T27 – see figure 2b for location of profiles. Successively, from inland oceanwards are shown: the atoll island, the reef flat zone bounded outwards by an algal ridge, the spur-and-groove

system (terrace TL1), two identified terrace lines, TL2 and TL3, respectively at depths of about −10 m and −14 m, an expected terrace line TL4, at about −20 m ending into a drop-off about 15 m high.

Fig. 7. Depth location of terraces identified from each bathymetric profile along the fore-reef slopes at Takapoto. A total of 112 individual terraces, including 96 well-defined and 16 expected, were counted. These are distributed among 7 terrace levels, at recurrent depths of about −5 m, −10 m, −15 m, −20 m, −24 m, −30.5 m, and −38 m.

Fig. 8. Google Earth Pro aerial view of a portion of the eastern atoll margin, showing from the rim seawards, the outer reef-flat zone, algal reef crest, spur-and-groove system (terrace TL1), gently dipping terrace TL2 abruptly ending into dark waters.

Fig. 9. Relative frequency and percentage of terraces plotted by width range, and calculated from 112 terraces identified from levels TL 2 to TL7.
The histogram is left-skewed, expressing high frequency of terraces less than 15 m wide.

Fig. 10. Plot of terrace width as a function of the detected length of bathymetric profiles.
Are plotted 112 terraces identified from levels TL2 to TL7.

Fig. 11. Close-up pictures of coral communities at different depths from −5 m to −30 m, fore-reef slope, Fakatopatere area, south end of Takapoto.

(a) −5 m depth: spur surface partly covered by robust branching *Pocillopora* (*P. verrucosa*).

(b) −10 m depth: terrace colonized by coral head mostly composed of *Pocillopora verrucosa*, together with some branching, cluster-like *Pocillopora elegans*.

(c) −15 m depth: up to 1 m, thick coral cover, mainly composed of plate-shaped to encrusting colonies of *Porites rus.*

(d) −20 m depth: coral patch dominated by plate-like *Porites rus*.

(e) and (f): −25 m and −30 m deep: drop-offs densely encrusted by plate-like *Porites rus*.

Fig. 12. Wide-angle view of drop-offs between −28 m and −32 m, showing dense cover of *Porites rus*.

Fig. 13. Depth ranges of terrace levels (TL1 to TL6) identified from fore-reef slopes at Takapoto, compared with stratigraphic position of surface unconformities in interpretative core sections from Moruroa, Enewetak, Bikini, Tarawa, and Yongle atolls. Absolute dates are indicated locally on the right side of Moruroa, Enewetak, and Tarawa cores.

Fig. 14. Eustatic sea level curve for the last 350 ky (from Grant et al., 2014) with position of terrace levels (TL1 to TL6) identified from fore-reef slopes at Takapoto.

Symbols for terrace levels: red coloured = present-day depth range; green coloured = former depth range after correction of subsidence and ground lowering.

Correspondance between terrace levels and marine isotope stages: TL1 = MIS 1; TL2 = MIS 5e; TL3 = MIS 7a; TL4 = MIS 7c; TL5 = MIS 7e; TL6 = MIS 9e.

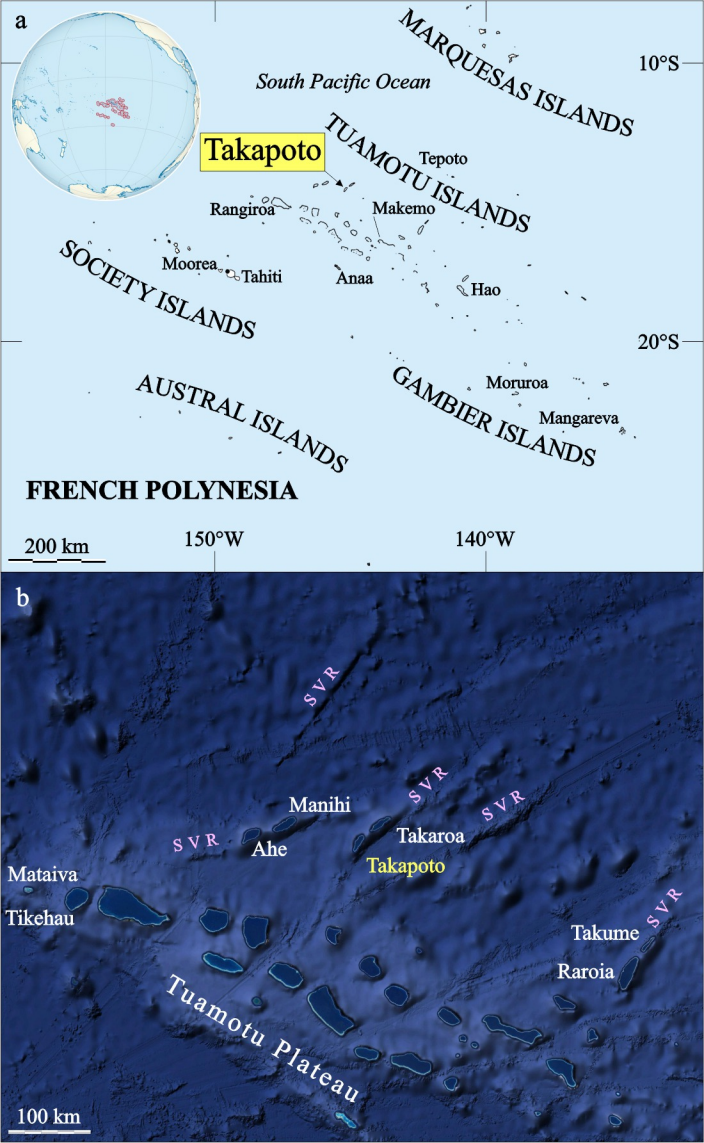
a
MARQUESAS ISLANDS
10°S
South Pacific Ocean
Takapoto
TUAMOTU ISLANDS
Tepoto
Rangiroa
Makemo
Moorea
Tahiti
Anaa
Hao
SOCIETY ISLANDS
20°S
AUSTRAL ISLANDS
GAMBIER ISLANDS
Moruroa
Mangareva
FRENCH POLYNESIA
200 km
150°W
140°W
b
SVR
SVR
SVR
SVR
Manihi
Ahe
Takaroa
Takapoto
Mataiva
Tikehau
Takume
SVR
Raroia
Tuamotu Plateau
100 km

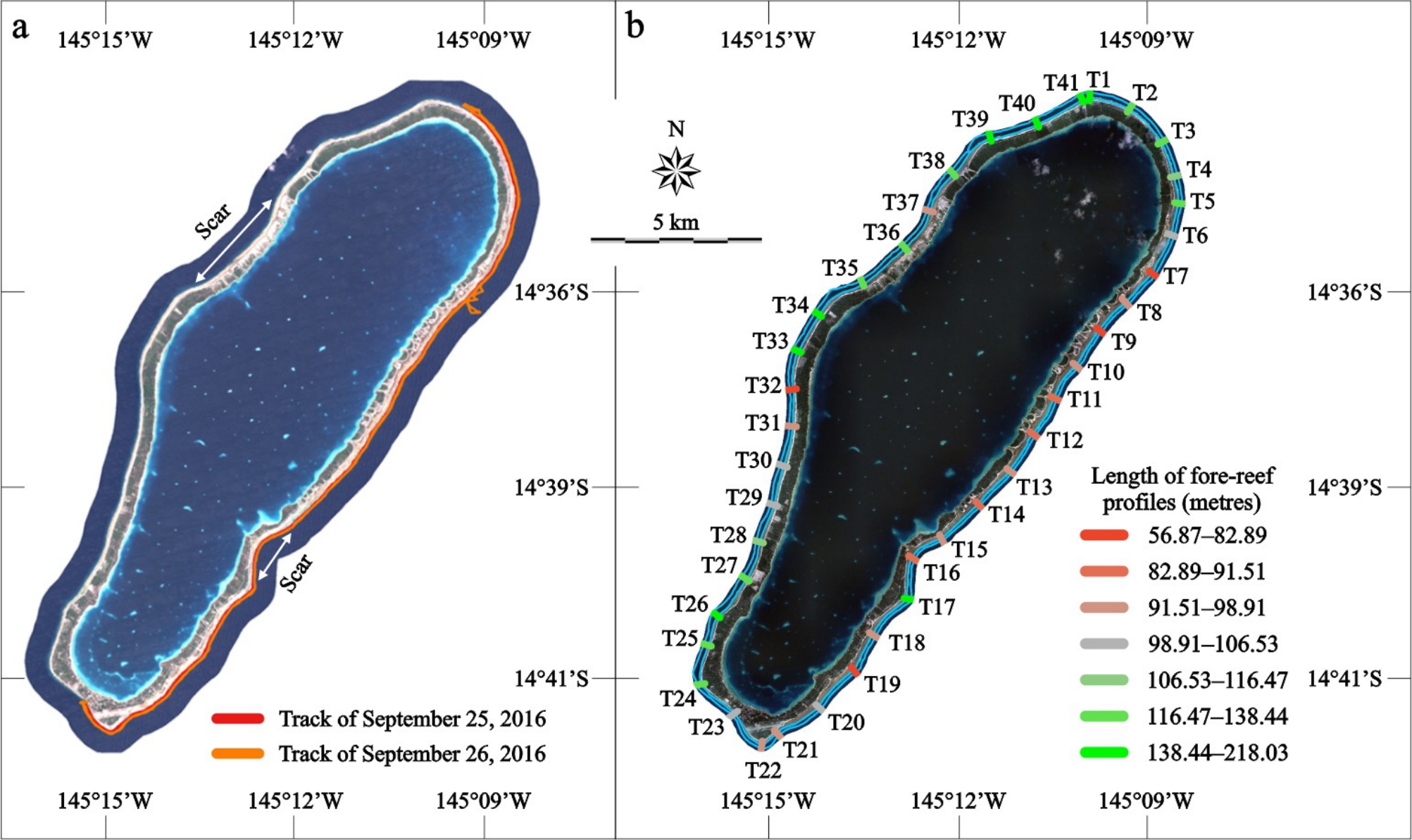
a
145°15'W
145°12'W
145°09'W
14°36'S
14°39'S
14°41'S
Scar
Scar
Track of September 25, 2016
Track of September 26, 2016
b
N
5 km
T1
T2
T3
T4
T5
T6
T7
T8
T9
T10
T11
T12
T13
T14
T15
T16
T17
T18
T19
T20
T21
T22
T23
T24
T25
T26
T27
T28
T29
T30
T31
T32
T33
T34
T35
T36
T37
T38
T39
T40
T41
Length of fore-reef profiles (metres)
56.87–82.89
82.89–91.51
91.51–98.91
98.91–106.53
106.53–116.47
116.47–138.44
138.44–218.03

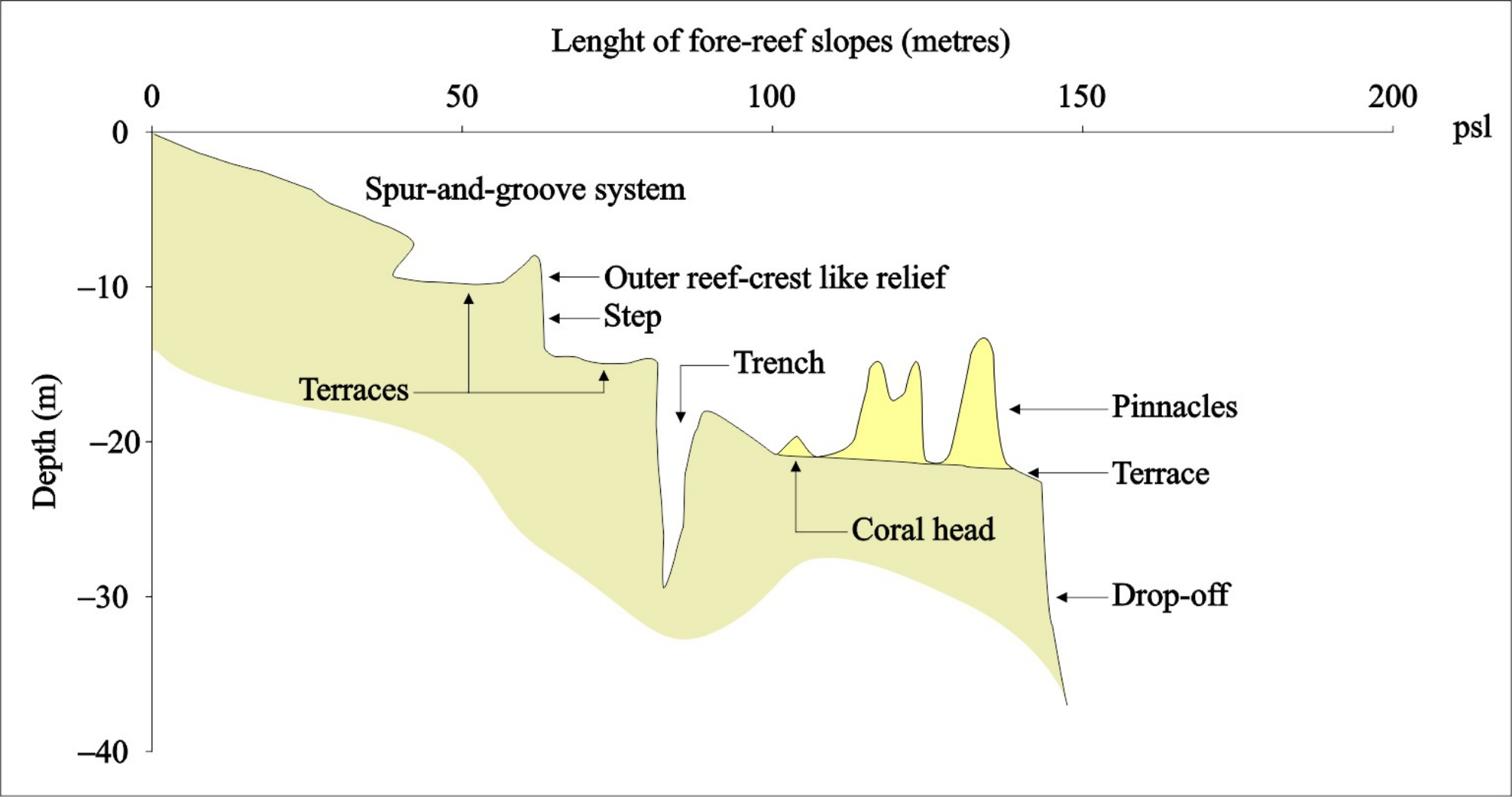
Lenght of fore-reef slopes (metres)
0
50
100
150
200
psl
0
–10
–20
–30
–40
Depth (m)
Spur-and-groove system
Outer reef-crest like relief
Step
Trench
Terraces
Pinnacles
Terrace
Coral head
Drop-off

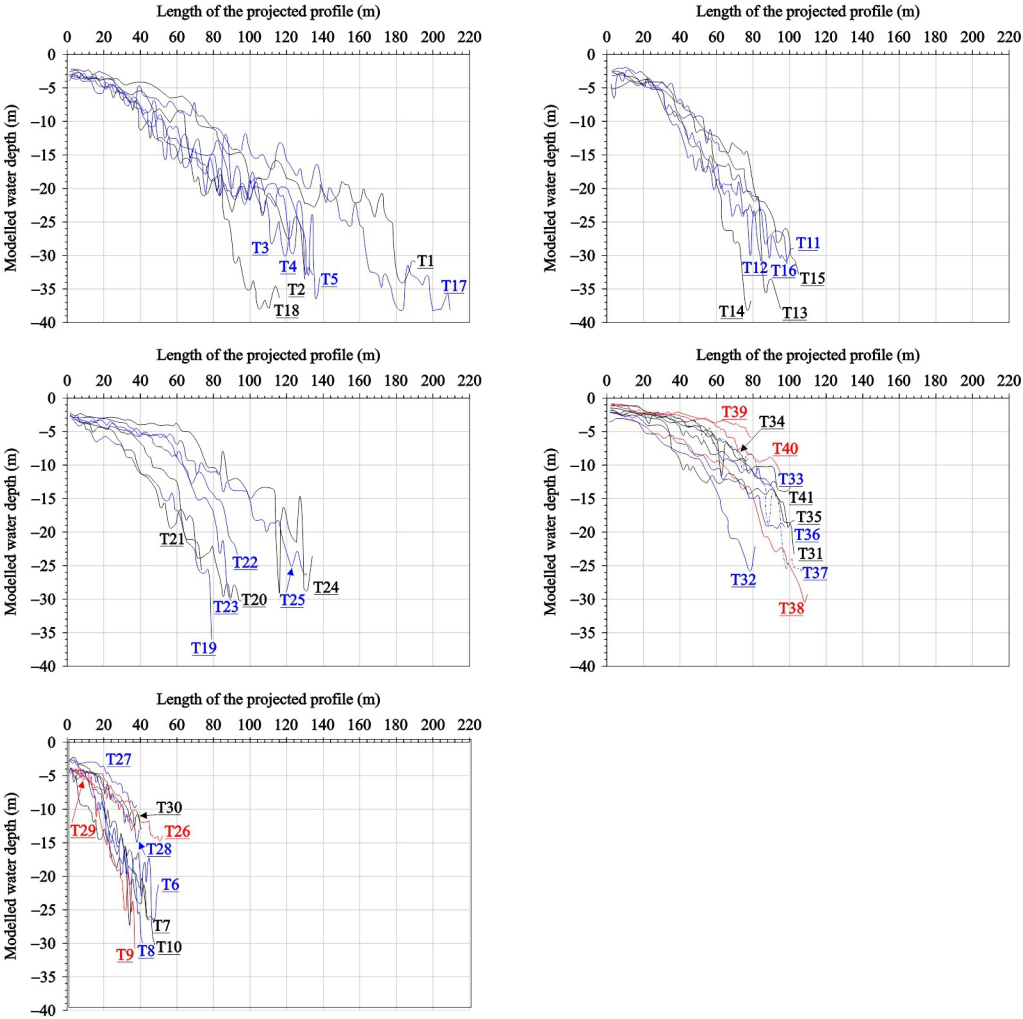
Length of the projected profile (m)
Modelled water depth (m)
T1
T2
T3
T4
T5
T17
T18
T11
T12
T13
T14
T15
T16
T19
T20
T21
T22
T23
T24
T25
T31
T32
T33
T34
T35
T36
T37
T38
T39
T40
T41
T6
T7
T8
T9
T10
T26
T27
T28
T29
T30

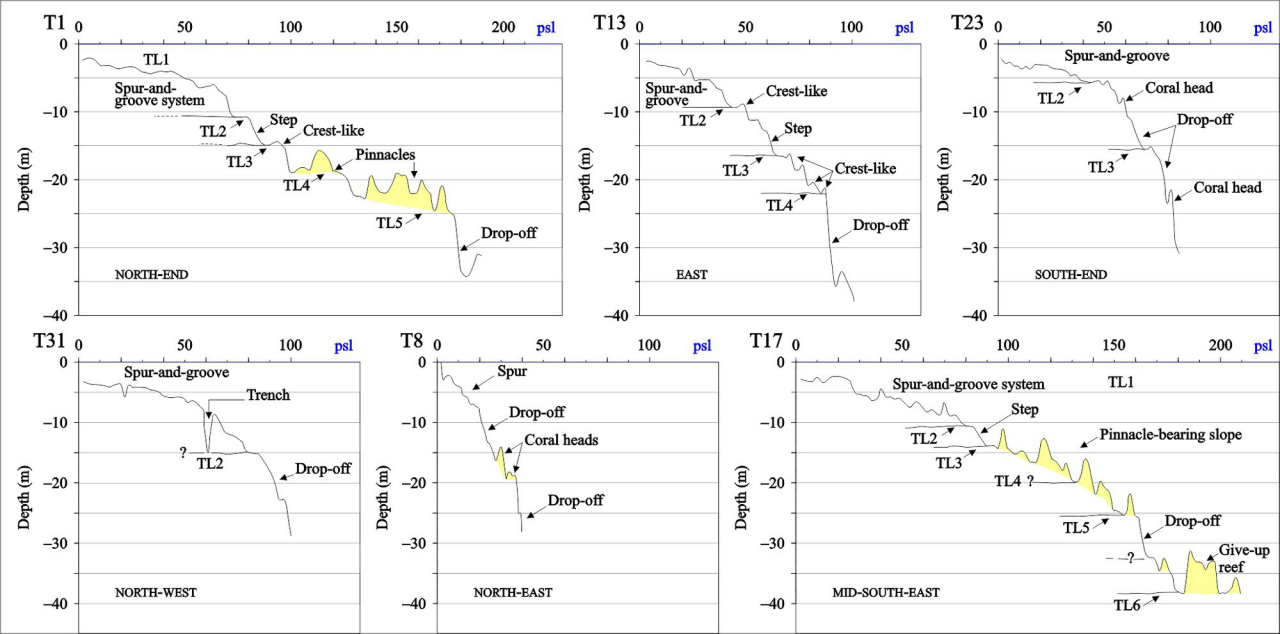
T1
psl
Depth (m)
TL1
Spur-and-groove system
Step
TL2
Crest-like
TL3
Pinnacles
TL4
TL5
Drop-off
NORTH-END
T13
Spur-and-groove
Crest-like
TL2
Step
TL3
Crest-like
TL4
Drop-off
EAST
T23
Spur-and-groove
Coral head
TL2
Drop-off
TL3
Coral head
SOUTH-END
T31
Spur-and-groove
Trench
?
TL2
Drop-off
NORTH-WEST
T8
Spur
Drop-off
Coral heads
Drop-off
NORTH-EAST
T17
Spur-and-groove system
TL1
Step
TL2
Pinnacle-bearing slope
TL3
TL4 ?
TL5
Drop-off
?
Give-up reef
TL6
MID-SOUTH-EAST

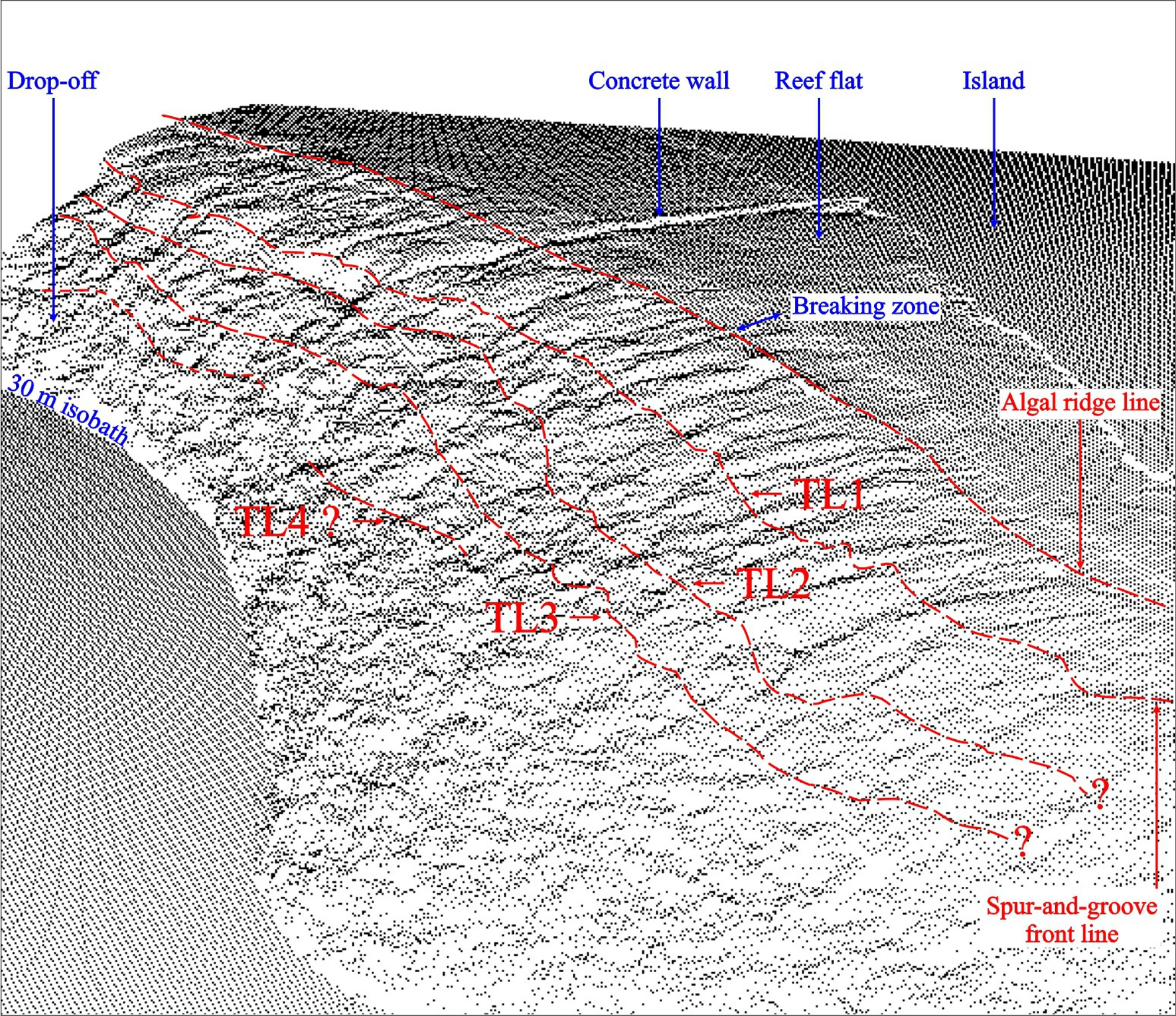
Drop-off
Concrete wall
Reef flat
Island
Breaking zone
30 m isobath
Algal ridge line
TL1
TL2
TL3
TL4 ?
?
?
Spur-and-groove
front line

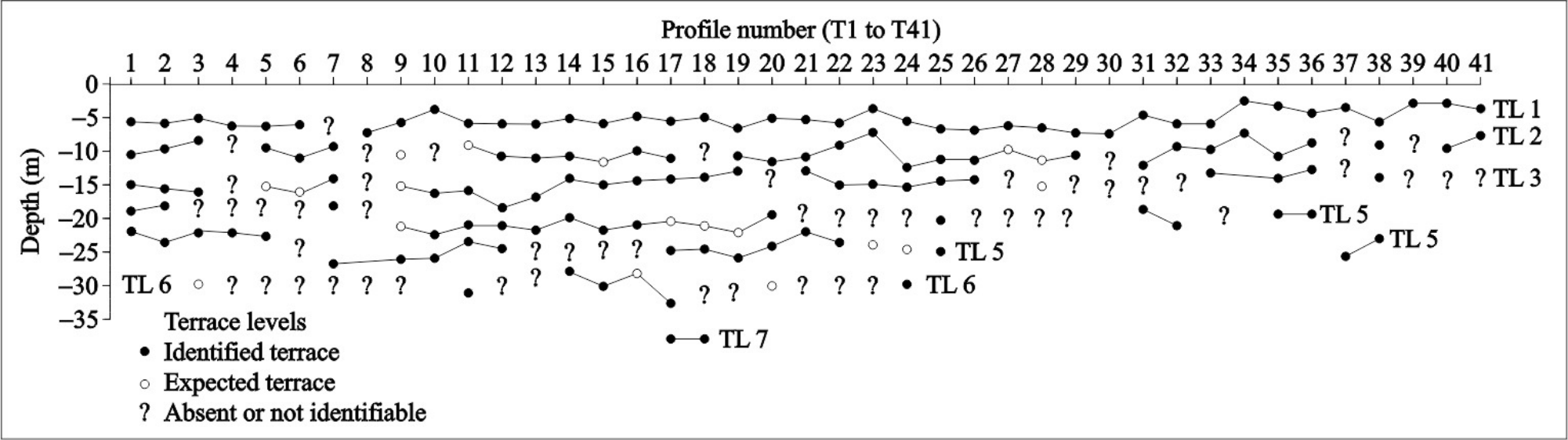
Profile number (T1 to T41)
1 2 3 4 5 6 7 8 9 10 11 12 13 14 15 16 17 18 19 20 21 22 23 24 25 26 27 28 29 30 31 32 33 34 35 36 37 38 39 40 41
Depth (m)
0
−5
−10
−15
−20
−25
−30
−35
TL 1
TL 2
TL 3
TL 5
TL 5
TL 5
TL 6
TL 6
TL 7
Terrace levels
Identified terrace
Expected terrace
? Absent or not identifiable

Reef flat
Algal reef crest
Spur-and-groove system – TL1
TL2
Shelf slope
145°13'33.63W
14°41'51.06S
N
20 m

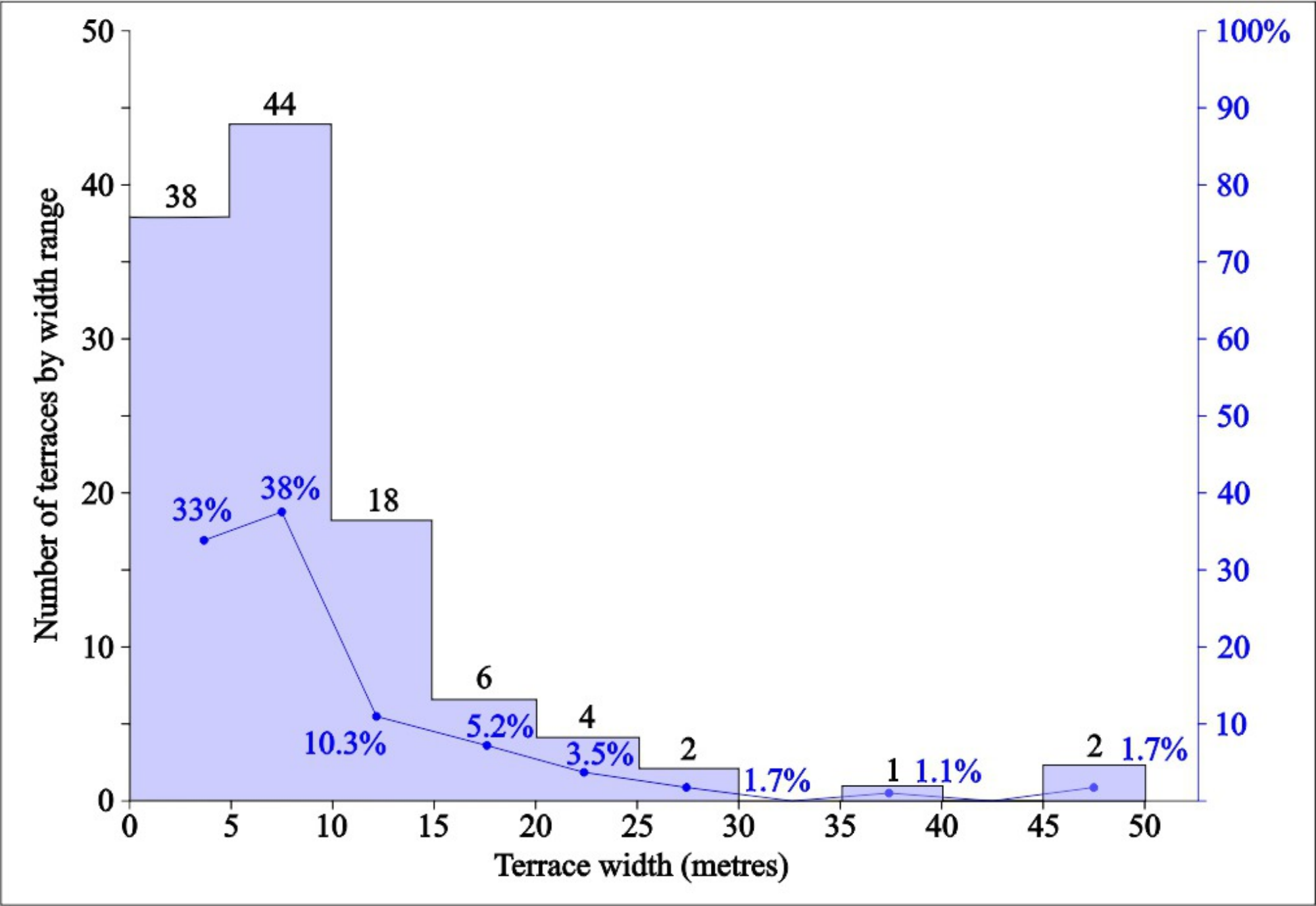
Number of terraces by width range
Terrace width (metres)
0
10
20
30
40
50
0
5
10
15
20
25
30
35
40
45
50
10
20
30
40
50
60
70
80
90
100%
38
44
18
6
4
2
1
2
33%
38%
10.3%
5.2%
3.5%
1.7%
1.1%
1.7%

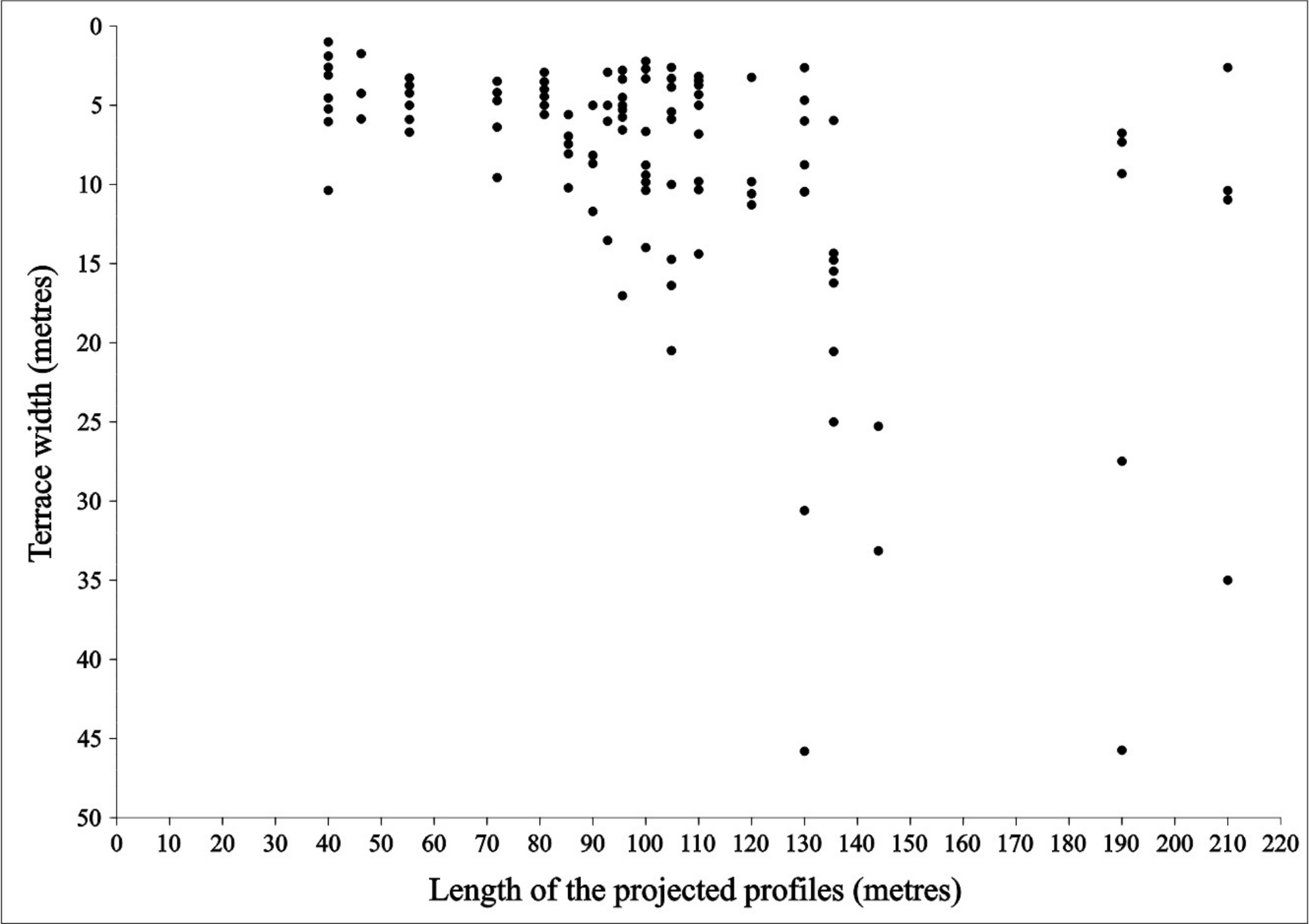
Terrace width (metres)
0
5
10
15
20
25
30
35
40
45
50
0
10
20
30
40
50
60
70
80
90
100
110
120
130
140
150
160
170
180
190
200
210
220
Length of the projected profiles (metres)

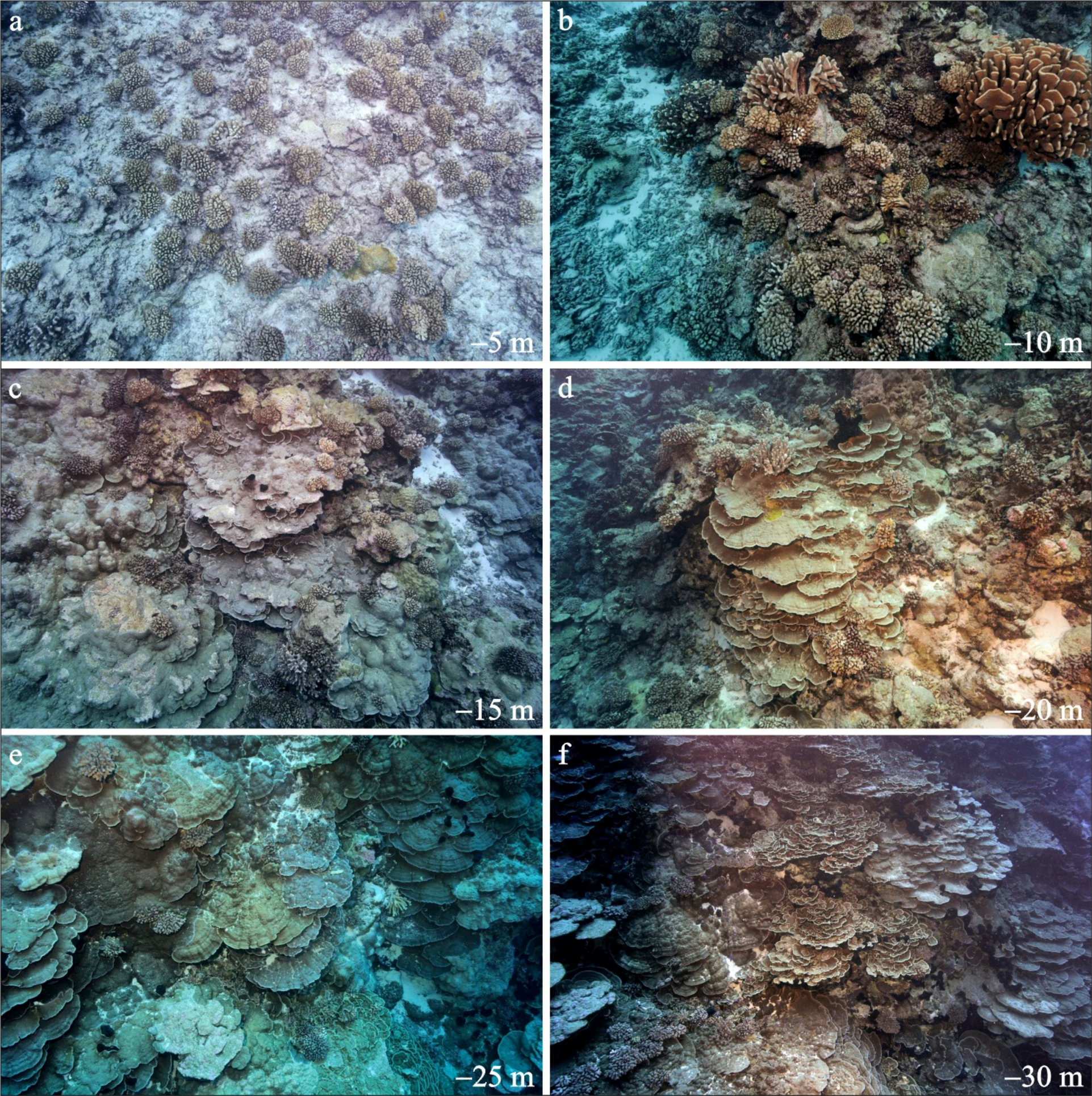
a
–5 m
b
–10 m
c
–15 m
d
–20 m
e
–25 m
f
–30 m

–30 m

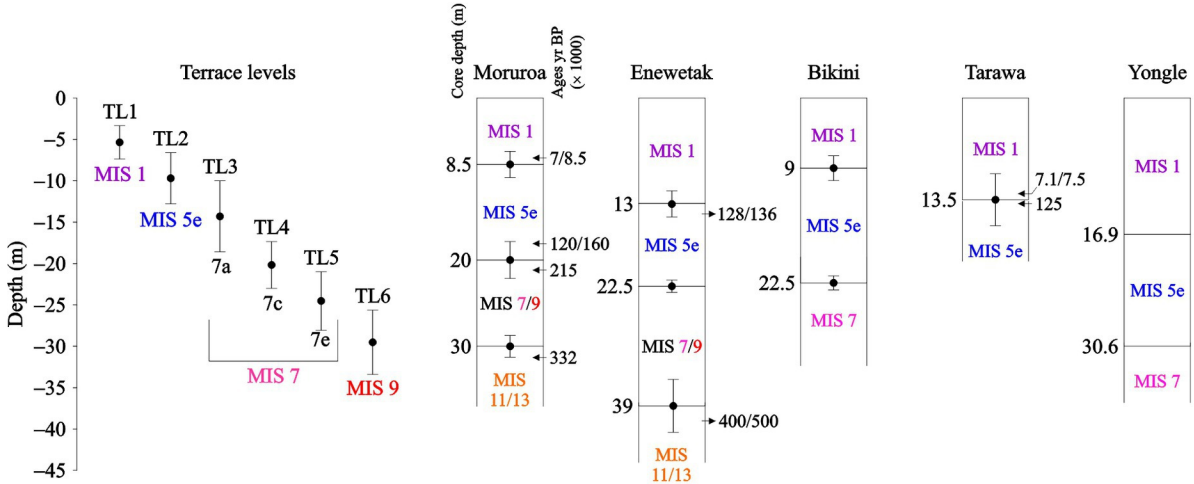
Terrace levels
Depth (m)
0
−5
−10
−15
−20
−25
−30
−35
−40
−45
TL1
TL2
TL3
TL4
TL5
TL6
MIS 1
MIS 5e
7a
7c
7e
MIS 7
MIS 9
Core depth (m)
Ages yr. BP (× 1000)
Moruroa
MIS 1
8.5
7/8.5
MIS 5e
20
120/160
215
MIS 7/9
30
332
MIS 11/13
Enewetak
MIS 1
13
128/136
MIS 5e
22.5
MIS 7/9
39
400/500
MIS 11/13
Bikini
MIS 1
9
MIS 5e
22.5
MIS 7
Tarawa
MIS 1
13.5
7.1/7.5
125
MIS 5e
Yongle
MIS 1
16.9
MIS 5e
30.6
MIS 7

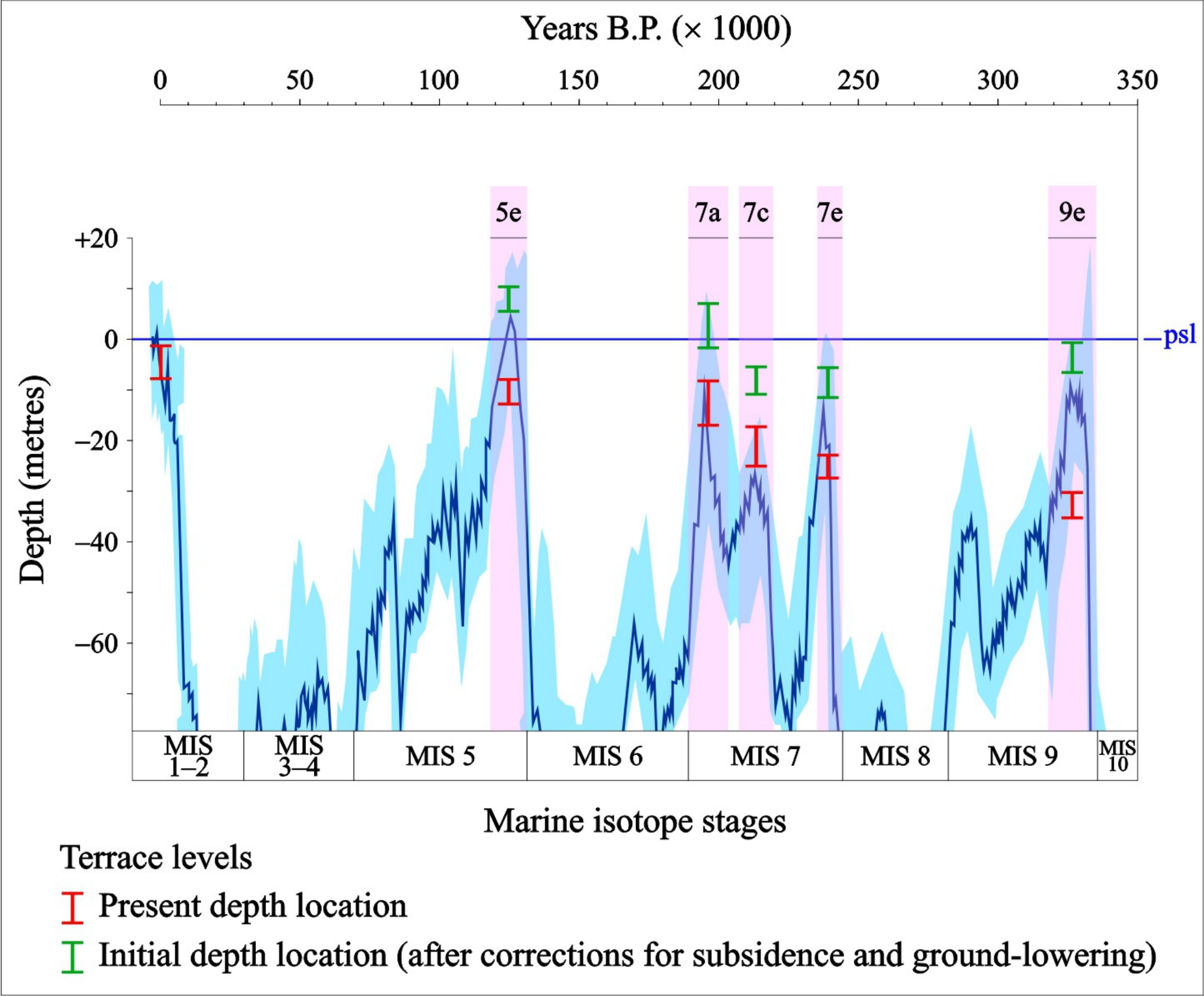
Years B.P. (× 1000)
0
50
100
150
200
250
300
350
5e
7a
7c
7e
9e
+20
0
−20
−40
−60
Depth (metres)
psl
MIS 1–2
MIS 3–4
MIS 5
MIS 6
MIS 7
MIS 8
MIS 9
MIS 10
Marine isotope stages
Terrace levels
Present depth location
Initial depth location (after corrections for subsidence and ground-lowering)

Types	Definitions
Fore-reef zone	the area extending from the seaward margin of the atoll rim to the deepest detected isobath
Shelf slope	the area extending beyond the lowest limits of the spur-and-groove system (−10 m deep on average) to the deepest detected isobaths
Reef edge	the outermost, top part of a reef tract
Spur-and-groove system	the uppermost part of a fore-reef zone formed by a series of parallel, linear ridges (spurs) alternating with narrow channels (grooves), oriented perpendicular to the reef-crest line and extending down to average depths of −10 m
Terrace	a relatively flat-topped or gently dipping surface, which is bounded seawards by a steeper descending slope or step and inwards by a steeper ascending slope
Outer-reef crest like-relief	about 1 m-high, strictly located to the seaward outer margin of a reef tract or terrace
Drop-off	a relatively high (up to 10 m), vertical surface facing the open sea
Step	a low (less than 10 m), steeply inclined to vertical surface, and usually located at the seaward end of a terrace
Pinnacle	an isolated, composite, tower-shaped relief up to 2 m high, both terraces and slopes
Coral head	a relief less than 2 m high, occasionally composed of one single large colonies, but usually composite in nature, located at different places on terraces and slopes
Trench	narrow, vertical cut deeply dissecting the fore-reef zone
Scar	bight-shaped indentations along the outer reef margin

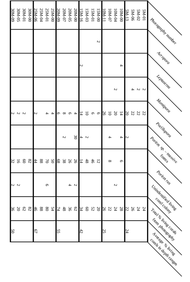

Terrace levels	Present depth (m)	Expected MIS stages	Time duration (ky)	Reflooding time (ka)	duration of emergence (ky)	Amplitude of ground lowering (m)	Amplitude of subsidence (m)	Deepening of terraces (m)	Past sea-level elevation (m)
TL3	14.7 ± 3.8	7a	–201.5 to –189.7	128	61.7	7.4	9.5	16.9	2.0 ± 3.8 apsl
TL4	20.3 ± 2.3	7c	–217.2 to –206.0	196	10.0	1.2	9.6	10.8	9.5 ± 2.3 bpsl
TL5	24.0 ± 2.0	7e	–248.9 to –231.0	(1) 220 (2) 200	11.0 31.0	1.3 3.7	11.7 11.7	13.0 15.4	11.0 ± 2.0 bpsl 8.6 ± 2.0 bpsl
TL6	30.5 ± 3.0	9	–335.6 to –316.8	240	76.8	9.2	15.8	25.0	5.5 ± 3.0

Rate of sub-aerial erosion = 0.12 mm/y
Rate of subsidence = 0.047 mm/y

(1) MIS 7e reef overlapped by MIS 7c reef
(2) No overlapping

apsl : above present sea-level
bpsl : below present sea-level